

AD-A031 784 SYRACUSE UNIV N Y DEPT OF ELECTRICAL AND COMPUTER E--ETC F/G 9/5
A REACTIVELY LOADED APERTURE ANTENNA ARRAY.(U)
SEP 76 J LUZWICK, R F HARRINGTON
UNCLASSIFIED TR-76-10

N00014-76-C-0225

NL

1 of 1
ADA031784



END

DATE
FILMED
12 - 76

ADA031784

UNCLASSIFIED

SECURITY CLASSIFICATION OF THIS PAGE (When Data Entered)

DD FORM 1 JAN 73 1473 EDITION OF 1 NOV 68 IS OBSOLETE
S/N 0102-014-6601

UNCLASSIFIED

1 SECURITY CLASSIFICATION OF THIS PAGE (When Data Entered)

406737

UNCLASSIFIED

SECURITY CLASSIFICATION OF THIS PAGE(When Data Entered)

→ considered explicitly. Feasibility for physical realization of the reactive loading is discussed. A computer program with operating instructions is included.



ACCESSION for	
NTIS	White Section <input checked="" type="checkbox"/>
DOC	Buff Section <input type="checkbox"/>
UNANNOUNCED	<input type="checkbox"/>
JUSTIFICATION	
.....	
BY	
DISTRIBUTION/AVAILABILITY CODES	
Dist.	AVAIL. and/or SPECIAL
A	

ACKNOWLEDGEMENT

Thanks are due to Dr. Joseph Mautz for his suggestions and critiques during the investigation.

CONTENTS

	Page
PART ONE - THEORY AND EXAMPLES	
I. INTRODUCTION-----	1
II. GENERAL FORMULATION-----	1
III. ADMITTANCE FORMULATION-----	12
IV. GAIN FORMULATION-----	17
V. REPRESENTATIVE COMPUTATIONS-----	20
VI. REALIZATION OF THE REACTIVE LOADS-----	21
VII. DISCUSSION AND CONCLUSIONS-----	28
PART TWO - COMPUTER PROGRAMS	
I. INTRODUCTION-----	33
II. ADMITTANCE MATRIX-----	33
III. MEASUREMENT VECTOR P^m -----	37
IV. MAXIMUM GAIN, COMPLEX AND REAL EQUIVALENT VOLTAGE SOURCES, ALL APERTURES FED-----	39
V. RESONANT LOADS-----	44
VI. GAIN PATTERNS-----	46
VII. EIGENVALUE DETERMINATION-----	50
VIII. MAIN PROGRAM AND SAMPLE INPUT-OUTPUT DATA-----	53
REFERENCES-----	63

PART ONE
THEORY AND EXAMPLES

I. INTRODUCTION

In a previous report [1], it was demonstrated that for linear and circular arrays of dipoles the radiation characteristics can be controlled by using a single feed and reactively loading the other dipoles. By varying the load reactances, the antenna beam can be steered.

This report uses a similar technique applied to a waveguide-backed aperture array. Only one aperture is excited. The remaining apertures are reactively loaded by placing electrical short circuits in waveguides at variable distances from the apertures (see Fig. 1). An important advantage of this design is a reduction in the number of direct-fed elements in an aperture array.

Coe and Held [2] considered a similar problem which involved the dual of the YAGI-UDA linear antenna array using rectangular apertures (reflector, feed, and directors) in an infinite conducting ground plane. Their work was concerned primarily with radiation in the end-fire direction.

II. GENERAL FORMULATION

The basis for this formulation can be found in a previous report by Harrington and Mautz [3] which presents a general treatment of aperture problems. We first consider the problem of a single waveguide-backed aperture radiating into a half-space (see Fig. 2). The Equivalence Principle [4] is used to divide this problem into two separate regions as follows (see Fig. 3). The aperture is covered by an electric conductor. The fields in the waveguide region are produced by the impressed sources \underline{J}^1 , \underline{M}^1 , and the equivalent magnetic current \underline{M} where

$$\underline{M} = \underline{n} \times \underline{E} \quad (1)$$

over the aperture region with the aperture covered by an electric

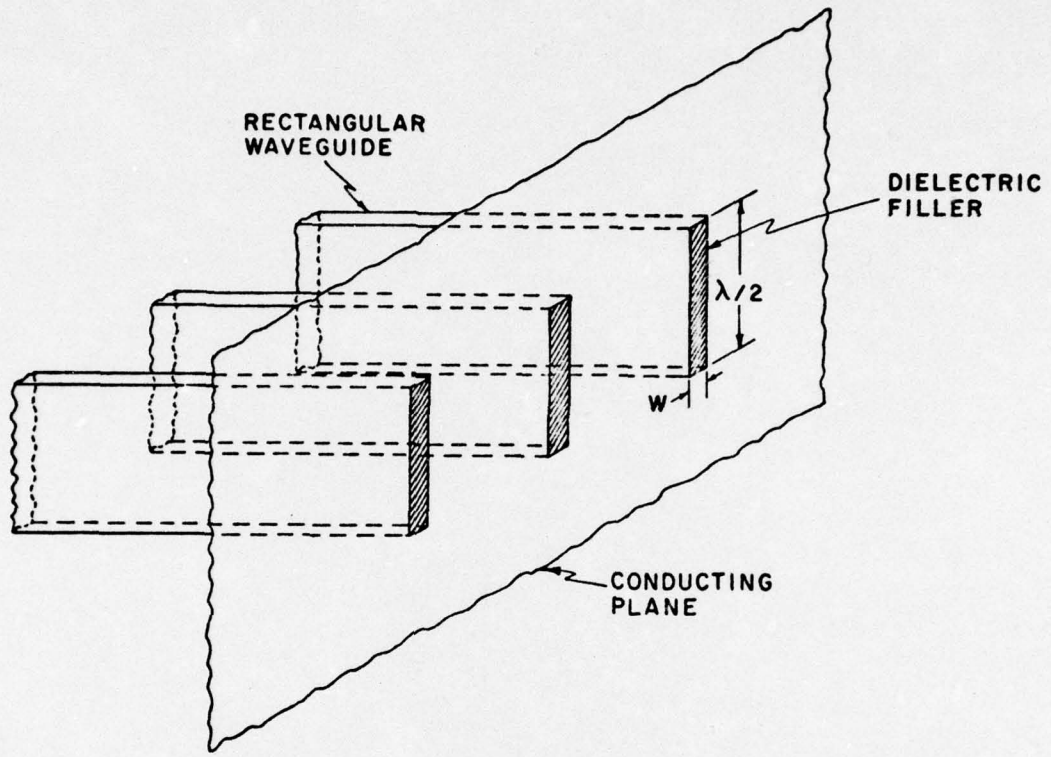


Fig. 1. An array of waveguide-backed apertures radiating into half space bounded by an electric conductor.

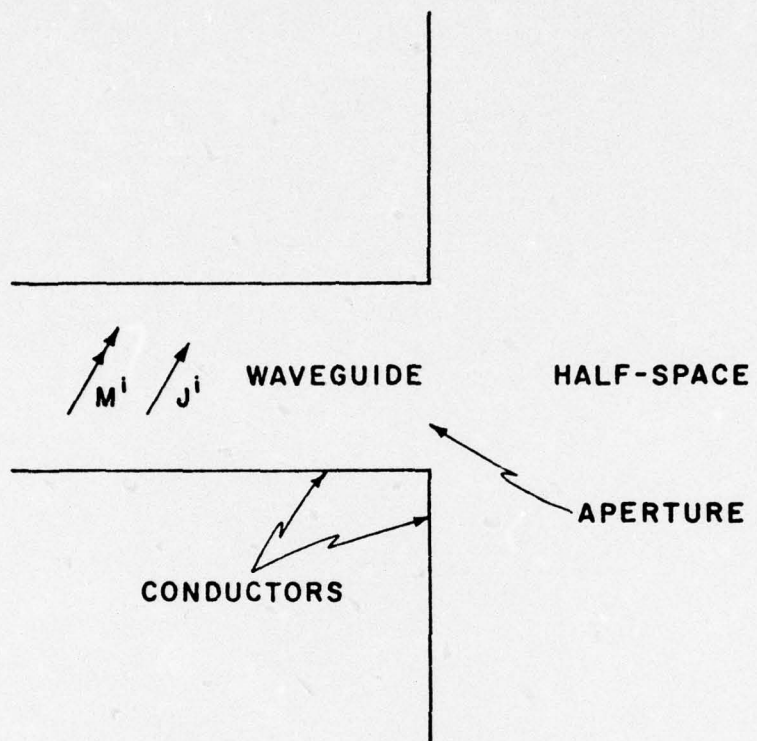


Fig. 2. A single waveguide-backed aperture radiating into half space bounded by an electric conductor.

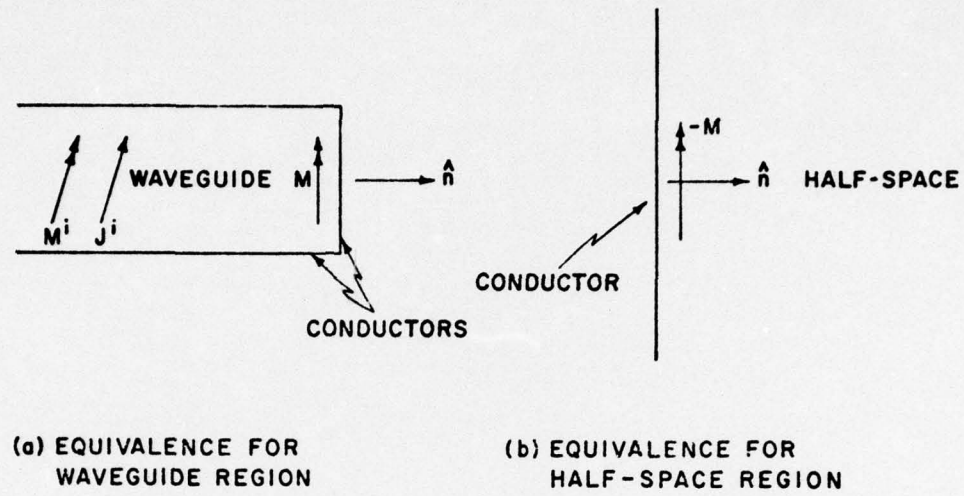


Fig. 3. The waveguide-backed aperture problem divided into two regions with equivalent sources.

conductor. The fields in the half-space region are produced by the equivalent magnetic current, $\underline{\underline{M}}$, with the aperture covered by an electric conductor. The fact that the equivalent magnetic current in the waveguide region is $\underline{\underline{M}}$ and in the half-space region $\underline{\underline{M}}$ ensures that the tangential component of electric field is continuous across the aperture.

Another necessary boundary condition is the continuity of the tangential component of magnetic field across the aperture. The tangential magnetic field over the aperture on the waveguide side, $\underline{\underline{H}}_{wt}^{wg}$, is equal to

$$\underline{\underline{H}}_{wt}^{wg} = \underline{\underline{H}}_{wt}^i + \underline{\underline{H}}_{wt}^{wg}(M) \quad (2)$$

where

$\underline{\underline{H}}_{wt}^i$ is the tangential magnetic field due to impressed sources

$\underline{\underline{H}}_{wt}^{wg}(M)$ is the tangential magnetic field due to the equivalent magnetic source M .

On the half-space side of the aperture we have

$$\underline{\underline{H}}_{ht}^{hs} = \underline{\underline{H}}_{ht}^{hs}(-\underline{\underline{M}}) = -\underline{\underline{H}}_{ht}^{hs}(M). \quad (3)$$

Note that $\underline{\underline{H}}_{wt}^i$, $\underline{\underline{H}}_{wt}^{wg}(M)$, and $\underline{\underline{H}}_{ht}^{hs}(M)$ are all computed with an electric conductor covering the aperture. A true solution is obtained when $\underline{\underline{H}}_{wt}^{wg}$ of (2) equals $\underline{\underline{H}}_{ht}^{hs}$ of (3), or

$$\underline{\underline{H}}_{wt}^{wg}(M) + \underline{\underline{H}}_{ht}^{hs}(M) = -\underline{\underline{H}}_{wt}^i. \quad (4)$$

Equation (4) is the defining relationship for determining the equivalent magnetic current M .

In reality, only an approximate solution of equation (4) can be obtained. The technique used in this report for solving equation (4) is the method of moments [5]. At this point in the formulation, we will extend our results to consider the multiple aperture case.

The extension from the single waveguide backed aperture problem to an array of waveguide-backed apertures with one waveguide fed is straightforward. Assume k (odd) apertures with the center aperture $(\frac{k+1}{2})$ driven. An electric conductor is placed over each aperture and the following boundary conditions are met (see Fig. 4)

$$\underline{H}_{\text{wg}}^{\text{wg}}(\underline{M}^i) + \sum_{j=1}^k \underline{H}_{\text{wg}}^{\text{hs}}(\underline{M}^j) = \begin{cases} 0 & i \neq \frac{k+1}{2} \\ -\underline{H}_t^i & i = \frac{k+1}{2} \end{cases}$$

$$i = 1, 2, \dots, k \quad (5)$$

where $\underline{H}_{\text{wg}}^{\text{wg}}(\underline{M}^i)$ is evaluated in the equivalent waveguide region and $\underline{H}_{\text{wg}}^{\text{hs}}(\underline{M}^j)$ in the equivalent half-space region of the i -th aperture. \underline{M}^j is the equivalent magnetic current \underline{M} in the j -th aperture region.

Now define

$$\underline{M}^j = u_y V_j M_j \quad (6)$$

where V_j is a complex constant to be determined and M_j is an expansion function to be specified. Substituting (6) into (5), we obtain

$$V_i \underline{H}_{\text{wg}}^{\text{wg}}(u_y M_i) + \sum_{j=1}^k V_j \underline{H}_{\text{wg}}^{\text{hs}}(u_y M_j) = \begin{cases} 0 & i \neq \frac{k+1}{2} \\ -\underline{H}_t^i & i = \frac{k+1}{2} \end{cases}$$

$$i = 1, 2, \dots, k \quad (7)$$

Next, we define a symmetric product

$$\langle A, B \rangle = \iint_{\text{aperture}} \underline{A} \cdot \underline{B} dS \quad (8)$$

and a testing function W_i in the i -th aperture region. Then, taking the symmetric product of (7) with each testing function, W_i , we obtain

$$V_i \langle W_i, \underline{H}_{\text{wg}}^{\text{wg}}(M_i) \rangle + \sum_{j=1}^k V_j \langle W_i, \underline{H}_{\text{wg}}^{\text{hs}}(M_j) \rangle = \begin{cases} 0 & i \neq \frac{k+1}{2} \\ -\langle W_i, H_t^i \rangle & i = \frac{k+1}{2} \end{cases}$$

$$i = 1, 2, \dots, k \quad (9)$$

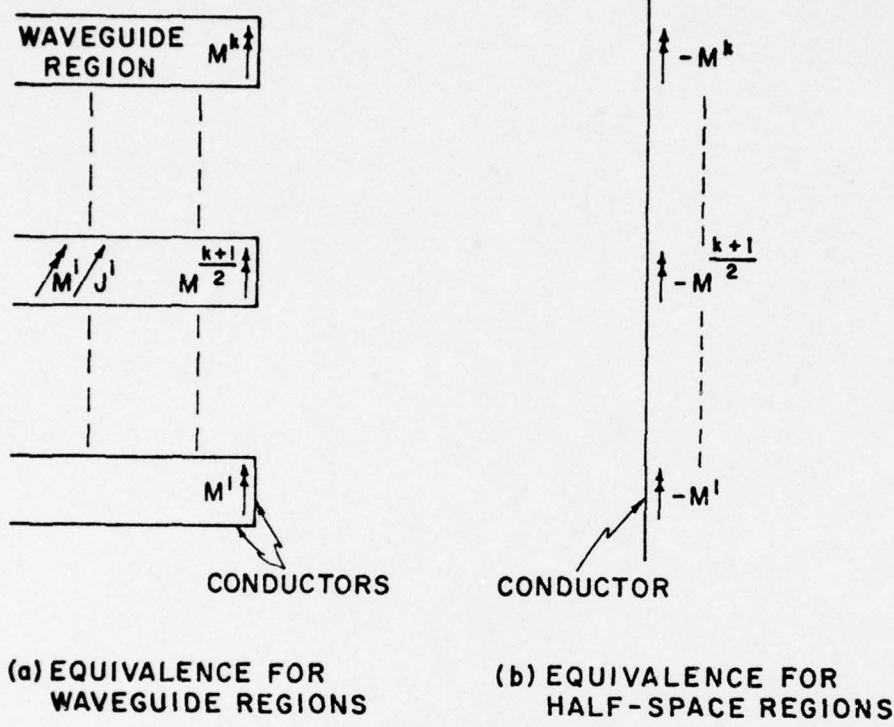


Fig. 4. The waveguide-backed aperture array problem divided into multiple regions with equivalent sources.

Solution of this set of linear equations determines the coefficients V_j and, therefore, the magnetic current M^j . Once M^j has been found, the field and field-related parameters can be computed.

Equation (9) can be rewritten in matrix notation as follows:
Define an admittance matrix for the waveguide regions as

$$[Y_{ii}^{wg}] = [\langle -W_i, H_{t_{ii}}^{wg}(M_i) \rangle] \quad (10)$$

and for the half-space regions as

$$[Y_{ij}^{hs}] = [\langle -W_i, H_{t_{ij}}^{hs}(M_j) \rangle] \quad (11)$$

where $H_{t_{ij}}^{hs}(M_j)$ is the tangential magnetic field in the i -th aperture region generated by the magnetic current in the j -th aperture region.
The minus sign is due to conventional power considerations. Define a source vector

$$\vec{I}^i = [\langle W_i, H_t^i \rangle]_{k \times 1} \quad (12)$$

and a coefficient vector

$$\vec{V} = [V_i]_{k \times 1}. \quad (13)$$

The resulting matrix equation which is equivalent to (9) is

$$[Y^{wg} + Y^{hs}] \vec{V} = \vec{I}^i. \quad (14)$$

The physical interpretation of (14) is that of two generalized admittance networks, $[Y^{wg}]$ and $[Y^{hs}]$, in parallel with the current source \vec{I}^i (see Fig. 5). By inverting (14), we obtain the resulting voltage vector which is the vector of coefficients which determines M

$$\vec{V} = [Y^{wg} + Y^{hs}]^{-1} \vec{I}^i \quad (15)$$

where

$$\vec{V} = \begin{bmatrix} V_1 \\ \vdots \\ V_k \end{bmatrix}, \quad \vec{I}^i = \begin{bmatrix} 0 \\ \vdots \\ I_{k+1} \\ \frac{I_2}{2} \\ \vdots \\ 0 \end{bmatrix}$$

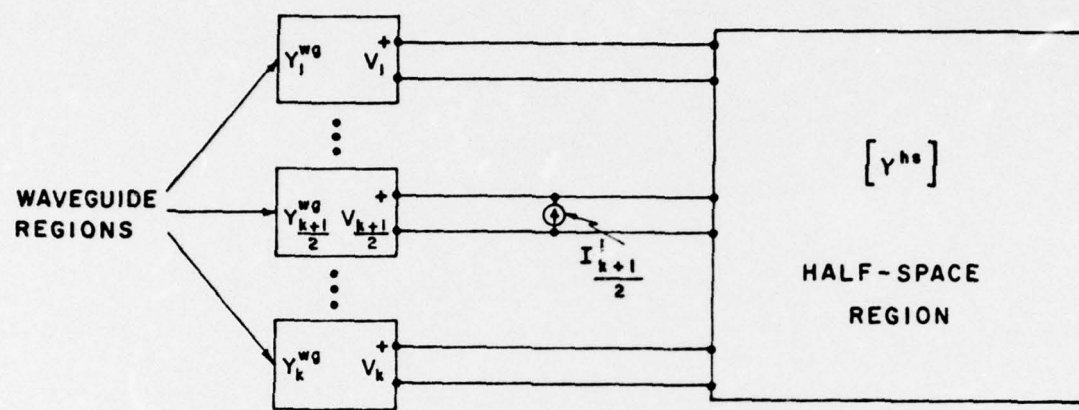


Fig. 5. The generalized network interpretation of equation (14).

$$[Y^{wg}] = \begin{bmatrix} Y_{11}^{wg} & & & \\ \cdot & \text{O} & & \\ \cdot & & \text{O} & \\ \cdot & & \cdot & Y_{kk}^{wg} \end{bmatrix}, \quad [Y^{hs}] = \begin{bmatrix} Y_{11}^{hs} & Y_{12}^{hs} & \dots & Y_{1k}^{hs} \\ Y_{21}^{hs} & Y_{22}^{hs} & & \\ \cdot & \cdot & \ddots & \\ \cdot & & & Y_{kk}^{hs} \end{bmatrix}.$$

An important result of this formulation is the separation of the original problem into two regions (waveguide and half-space) whose characteristics are defined by the admittance matrices, $[Y^{wg}]$ and $[Y^{hs}]$. Computation of $[Y^{wg}]$ involves only the waveguide region and $[Y^{hs}]$ only the half-space region. (One can see that a number of aperture boundary value problems can be solved by this equivalence formulation -- see reference [3].)

Now the following assumptions are made (see Fig. 6a):

1. The waveguides and apertures are one-half wavelength long.
2. The waveguides and apertures are filled with a dielectric ϵ_r .
3. Only the dominant mode exists in the waveguides and apertures.
4. The apertures are located on the x-axis with the long dimension in the y-direction.
5. There are an odd number of apertures.
6. A single expansion function represents the magnetic current covering each aperture region.

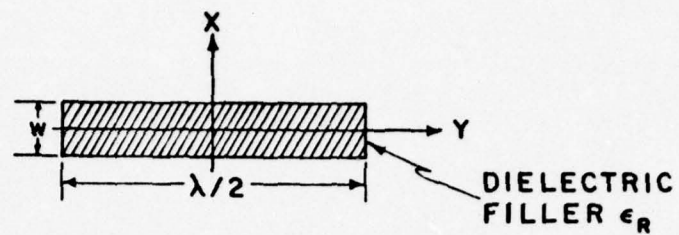
In addition to the preceding assumptions, the expansion (M_j) and testing (W_j) functions are defined as follows:

$$M_j = P_j(x) \cos ky \quad (15)$$

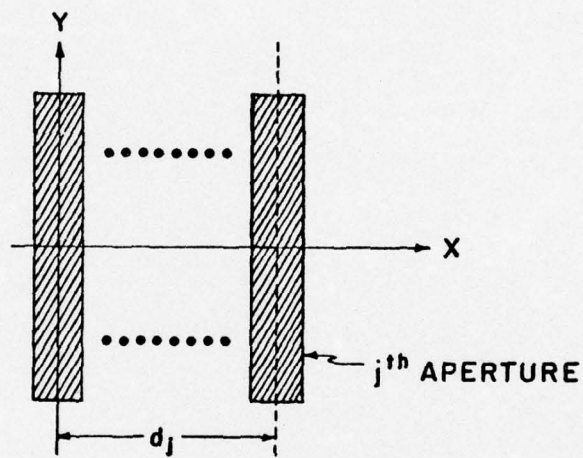
$$W_j = M_j = P_j(x) \cos ky \quad (16)$$

where

$$P_j(x) = \begin{cases} \sqrt{\frac{2}{wL}} & d_j - \frac{w}{2} \leq x \leq d_j + \frac{w}{2} \quad (\text{see Fig. 6b}) \\ 0 & \text{all other } x. \end{cases}$$



(a)



(b)

Fig. 6. Aperture geometry.

Substituting (15) and (16) into (10) and (11) we obtain

$$Y_{ii}^{wg} = \frac{2}{wL} \langle -\cos ky, H_{t_{ii}}^{wg} (\cos ky) \rangle \quad (17)$$

$$Y_{ij}^{hs} = \frac{2}{wL} \langle -\cos ky, H_{t_{ij}}^{hs} (\cos ky) \rangle . \quad (18)$$

III. ADMITTANCE FORMULATION

a) Determination of Y_{ii}^{wg} -

For the specific problem considered in this report, the waveguides are taken to be filled with a dielectric (ϵ_r), which lowers the cut-off frequency and allows the dominant mode cosine field to exist across the aperture.

For all of the waveguides except the externally driven one ($\frac{k+1}{2}$), we have

$$\begin{aligned} Y_{ii}^{wg} &= \frac{2}{wL} \langle -\cos ky, H_{t_{ii}}^{wg} (\cos ky) \rangle \\ &= -j Y_o \cot k_1 d^1(\phi), \quad i \neq \frac{k+1}{2} \end{aligned} \quad (19)$$

where $d^1(\phi)$ is the specific distance of the short circuit from the aperture in the i -th waveguide (dependent on beam steering angle ϕ)

k is the free-space wave number

k_c is the cut-off wave number

$$k_1 = \sqrt{\epsilon_r k^2 - k_c^2}$$

ϵ_r is the relative permittivity of the dielectric filler

η is the free-space intrinsic impedance

$$Y_o = \frac{1}{\eta} \sqrt{\epsilon_r - \left(\frac{k_c}{k}\right)^2}$$

Equation (19) is identical to the input admittance of a short-circuited transmission line where the characteristic admittance of the transmission line is replaced by the wave admittance of the dominant mode, Y_o . Physically, we have a waveguide excited at one end by an external field (mutual coupling) which is represented by an equivalent magnetic current source and short circuited at the other end (see Fig. 7).

For $i = \frac{k+1}{2}$ (externally driven waveguide), we have

$$\begin{aligned} Y_{ii}^{wg} &= \frac{2}{wL} \left\langle -\cos ky, H_{t_{ii}}^{wg} (\cos ky) \right\rangle \\ &= Y_o \text{ which is the wave admittance for the} \\ &\quad \text{dominant mode.} \end{aligned} \quad (20)$$

b) Determination of Y_{ij}^{hs} -

For evaluation of the off-diagonal elements of $[Y^{hs}]$, the equivalent magnetic current sheet in each aperture region is approximated by a filament of magnetic current, $WP(x) \cos ky$, at the center of the aperture (see Fig. 8(a)).

For evaluation of the diagonal elements of $[Y^{hs}]$, the concept of equivalent radius (see reference [6]) is used. This concept simply equates the characteristics of an aperture antenna to that of a cylindrical dipole with a radius $w/4$ (see Fig. 8(b)). Even though this equivalent radius is determined from a quasi-static principle, the admittance value obtained agrees quite closely to a time-harmonic derivation which solves for the admittance directly (see reference 7).

Now both diagonal and off-diagonal terms of the admittance matrix $[Y^{hs}]$ are in a form that can be evaluated using a dipole formulation. Y_{ij}^{hs} is proportional to Z_{ij} in [8 - equation 2-5]

$$\{Z_{ij}\} = - \int_{-L/2}^{L/2} E_{ij}(z) \frac{\sin k(\frac{L}{2} - |z|)}{\sin \frac{kL}{2}} dz$$

Therefore,

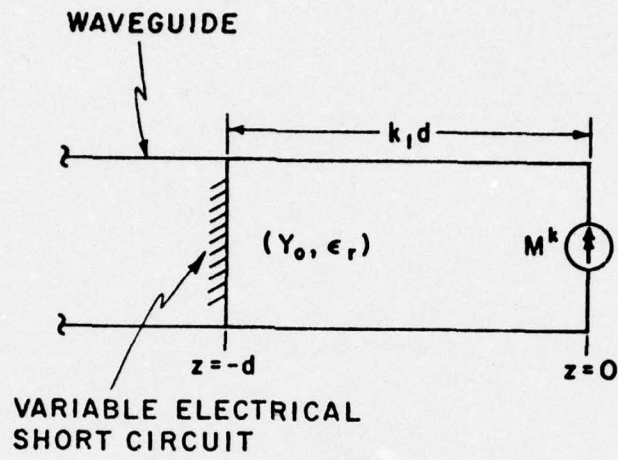
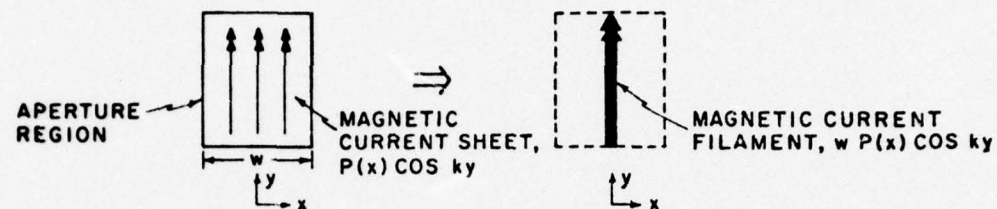
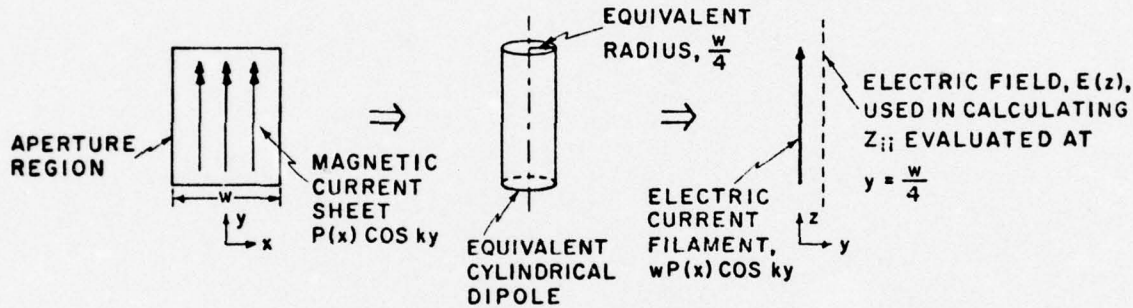


Fig. 7. The reactive load specified by equation (19).



(a) MAGNETIC CURRENT FILAMENT APPROXIMATION USED IN DETERMINING THE OFF-DIAGONAL COMPONENTS OF $[Y_{ij}^{hs}]$



(b) EQUIVALENT RADIUS AND MAGNETIC CURRENT FILAMENT APPROXIMATIONS USED IN DETERMINING DIAGONAL COMPONENTS OF $[Y_{ij}^{hs}]$

Fig. 8. Magnetic current source approximations used in the evaluation of diagonal and off-diagonal components of $[Y_{ij}^{hs}]$.

$$\begin{aligned}
 [Y_{ij}^{hs}] &= [\frac{2}{wL} \leftarrow \cos ky, H_{t_{ij}}^{hs} (\cos ky)] \\
 &= \frac{2}{\eta^2} \cdot \frac{2}{wL} \cdot w^2 \cdot [z_{ij}] \\
 &= \frac{4}{\eta^2} \cdot \frac{w}{L} \cdot [z_{ij}] . \tag{21}
 \end{aligned}$$

In the above equation, the first factor of 2 is due to imaging the magnetic current expansion function across the ground plane. The factor w^2 arises because both the expansion and testing magnetic current filaments are proportional to w . Finally, since the magnetic field due to a magnetic current is the same as the electric field due to an electric current with μ and ϵ interchanged, the factor $\frac{1}{\eta^2}$ is needed to reciprocate the factor η included in the expression for $E_{ij}(z)$ to obtain $H_{t_{ij}}^{hs}$. By incorporating the solution given for Z_{ij} in [8 - equation 2-7] into (21), we obtain

$$\begin{aligned}
 Y_{ij}^{hs} &= \frac{1}{\eta\pi} \left(\frac{w}{L} \right) [2 Ci(kd) - Ci(u_2) - Ci(v_2)] \\
 &\quad - \frac{1}{\eta\pi} \left(\frac{w}{L} \right) [2 Si(kd) - Si(u_2) - Si(v_2)] \tag{22}
 \end{aligned}$$

where $u_2 = k(\sqrt{d^2 + L^2} + L)$

$$v_2 = k(\sqrt{d^2 + L^2} - L)$$

$$Ci(x) = - \int_x^\infty \frac{\cos v}{v} dv$$

$$Si(x) = \int_0^x \frac{\sin v}{v} dv$$

$$i = j, d = \frac{w}{4}$$

$i \neq j$, d is the distance between the apertures i and j .

IV. GAIN FORMULATION

If the j -th waveguide is driven by an equivalent voltage source while all the other apertures are short circuited (therefore, acting like a continuous ground plane), a magnetic current \underline{M} will exist in the presence of an electric ground plane radiating into the half-space ($z > 0$). To determine the magnetic field at a point \underline{r}_m , consider the following analysis (see Figs. 9(a) and (b)).

By placing a magnetic dipole $K\underline{\ell}_m$ at \underline{r}_m and using reciprocity in terms of this field and the original field, we obtain the following equation

$$\underline{H}_m \underline{K}\ell_m = - \iint_{\text{aperture}} \underline{M} \cdot \underline{H}^m dS \quad (23)$$

where \underline{H}^m is the magnetic field from $K\underline{\ell}_m$ in the presence of a complete conductor and \underline{H}_m is the component in the direction of $K\underline{\ell}_m$ of the magnetic field at \underline{r}_m due to \underline{M} in the presence of a complete conductor. The magnetic current \underline{M} in (23) is generalized to the set of magnetic currents $\underline{u}_y V_i M_i$ in the i -th aperture to obtain

$$\begin{aligned} \underline{H}_m \underline{K}\ell_m &= \sum_i V_i \langle -M_i, H^m \rangle \\ &= \tilde{I}^m \vec{V} \quad i = 1, 2, \dots, k \end{aligned} \quad (24)$$

where \tilde{I}^m is the transpose of the measurement vector

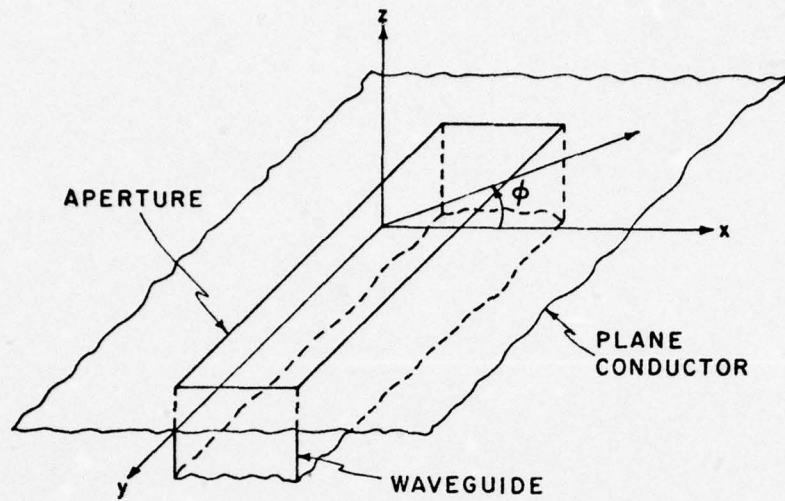
$$\tilde{I}^m = [\langle -M_i, H^m \rangle]_{k \times 1}. \quad (25)$$

Substituting (14) for \vec{V} in (24) we obtain

$$\underline{H}_m \underline{K}\ell_m = \tilde{I}^m [Y^{wg} + Y^{hs}]^{-1} \tilde{I}^m. \quad (26)$$

Now consider the following assumptions:

- (1) We adjust $K\underline{\ell}_m$ so that it produces a unit plane wave in the vicinity of the origin, that is,



(a) APERTURE ORIENTATION

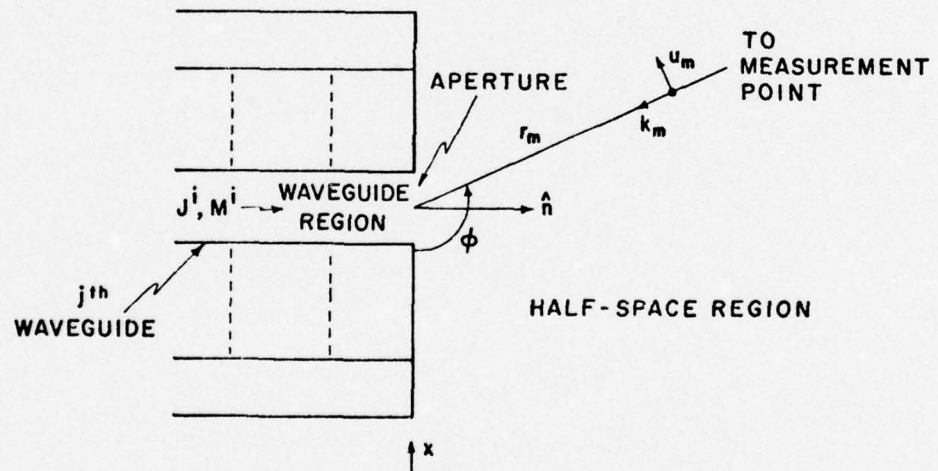
(b) MEASUREMENT VECTOR, P^m , GEOMETRY

Fig. 9. Waveguide-fed aperture in a plane conductor.

$$\frac{1}{K\ell_m} = \frac{-j\omega\epsilon}{4\pi r_m} e^{-jkr_m}. \quad (27)$$

(2) Define the far-field measurement vector as

$$\tilde{\mathbf{I}}_j^m = \tilde{\mathbf{P}}_j^m = -2 \iint_{\substack{j-\text{th} \\ \text{aperture}}} M_j \mathbf{u}_y \cdot \mathbf{u}_m e^{-jk\frac{r_m}{\lambda} \cdot \mathbf{r}} dS. \quad (28)$$

Substituting (27) and (28) into (26) we obtain

$$H_m = \frac{-j\omega\epsilon}{4\pi} \frac{e^{-jkr_m}}{r_m} \tilde{\mathbf{P}}^m [Y^{wg} + Y^{hs}]^{-1} \tilde{\mathbf{I}} \quad (29)$$

The complex power P_t transmitted through the aperture is

$$\begin{aligned} P_t &= \iint_{\text{aperture}} \mathbf{E} \times \mathbf{H}^* \cdot \hat{\mathbf{n}} dS \\ &= \iint_{\text{aperture}} M \cdot H^* dS. \end{aligned} \quad (30)$$

Since this transmitted power is only dependent on the tangential component of H in the half-space ($H_{it}^{hs} (-u_y M_j)$), equation (30) becomes

$$\begin{aligned} P_t &= - \sum_i \sum_j V_i V_j^* \iint_{\text{aperture}} M_i u_y \cdot (H_{it}^{hs}(-u_y M_j))^* dS \\ &= \sum_i \sum_j V_i V_j^* Y_{ij}^{hs*} \\ &= \tilde{V}[Y^{hs}]^* \tilde{V}^* \end{aligned} \quad (31)$$

$$i, j = 1, 2, \dots, k.$$

The gain (ratio of radiation intensity in a given direction to the radiation which would exist if the total power, P_t , were radiated

uniformly over the half-space) associated with the \hat{u}_m component of the magnetic field in the half-space ($z > 0$) is given by

$$G = \frac{2\pi r_m^2 n |H_m|^2}{\text{Real}(P_t)} . \quad (32)$$

By substitution of P_t and H_m into (32), we obtain

$$G = \frac{k^2}{8\pi n \text{Real}(\tilde{V}[Y^{hs}]^* \tilde{V}^*)} |\tilde{P}^m V|^2 \quad (33)$$

where

a) For E-plane patterns -

$$\begin{aligned} P_E^m &= -2 \sqrt{\frac{2}{WL}} \int_{-w/2+x_j}^{+w/2+x_j} e^{jkx} \cos \phi dx \int_{-\lambda/4}^{\lambda/4} \cos ky dy \\ &= \frac{-4\sqrt{2}}{k} \sqrt{\frac{w}{L}} e^{jkx_j} \cos \phi \left(\frac{\sin \left(\frac{kw}{2} \cos \phi \right)}{\frac{kw}{2} \cos \phi} \right) \end{aligned} \quad (34)$$

b) For H-plane patterns -

$$\begin{aligned} P_H^m &= -2 \sqrt{\frac{2}{WL}} w(-\sin \theta) \int_{-\lambda/4}^{\lambda/4} e^{jky} \cos \theta \cos ky dy \\ &= \frac{4\sqrt{2}}{k} \sqrt{\frac{w}{L}} \frac{\cos \left(\frac{\pi}{2} \cos \theta \right)}{\sin \theta} \end{aligned} \quad (35)$$

Note: θ is measured from the positive y axis in the $x=0$ plane.

V. REPRESENTATIVE COMPUTATIONS

A computer program has been written using the preceding derived equations. This program is described and listed in Part Two of this report. For this section, results will be given for $N=7$ and $N=9$ aperture arrays.

For the initial reactive loads, those which resonated complex and real equivalent sources were tried. In the $\phi = 0^\circ$ case, each required about the same amount of CPU time, while at $\phi = 30^\circ$, 60° and 90° , the loads which resonate complex equivalent sources required fewer iterations to achieve a maximum. In every case, the same end point was realized.

Figure 10 illustrates the maximum gain case for N=7 aperture array. If all the apertures are fed, maximum gain can be obtained since we have complete control over the complex source for each aperture. The disadvantage of this case lies in the excitation. A multiple feed network is required to realize the various complex excitations which are dependent on the beam steering angle ϕ .

Figure 11 illustrates the maximum gain that can be obtained using a single feed and reactive loads. The main advantage of this technique is the elimination of the complex rf feed networks used in the former case. Reduced controllability of the gain characteristics is the penalty that is paid by using this form of excitation. The results for this case were computed for $d_j = 0.27\lambda$ which is in a higher Q region of operation for the array.

Figure 12 illustrates the same number of apertures but in a lower Q (greater usable bandwidth) region of operation. The beamwidth is exceptionally high at $\phi = 30^\circ$ but becomes more satisfactory at greater beam steering angles. At the present time, this result would appear to restrict the useful scanning region for a practical Q and beamwidth.

Figure 13 illustrates the N=9 aperture case. The gain characteristics appear satisfactory except for the back lobe direction ($\phi = 180^\circ$) at low beam steering angles.

VI. REALIZATION OF THE REACTIVE LOADS

The reactive load as specified by equation (9) is short circuit terminating a transmission line. It can be realized using a variety of techniques. One of the simplest realizations is a sliding electrical conductor in a waveguide. This technique would be advantageous if it were desired to point the antenna beam in a fixed direction.

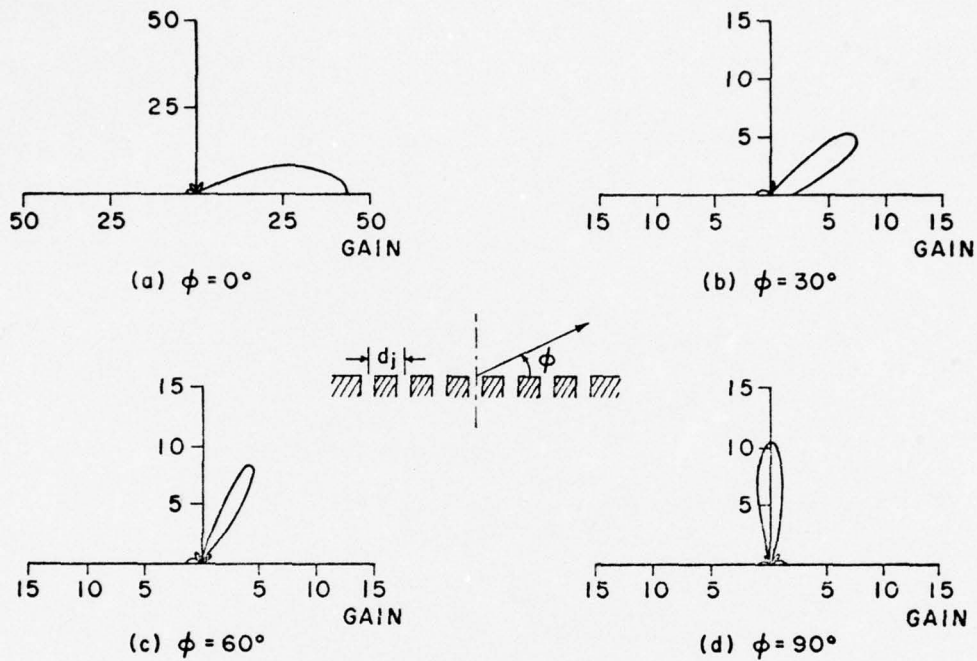


Fig. 10. Radiation gain patterns for a seven element aperture array when all elements are driven by the complex equivalent voltages which yield maximum gain, $d_j = 0.27\lambda$.

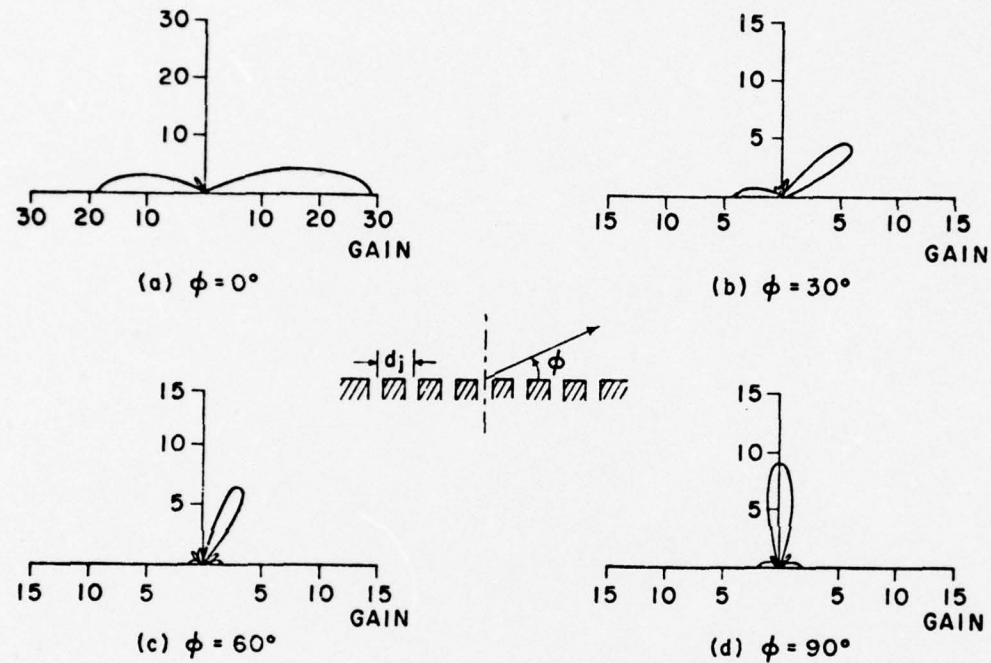


Fig. 11. Radiation gain patterns for a seven element reactively loaded aperture array when only the center aperture is externally driven, $d_j = 0.27\lambda$.

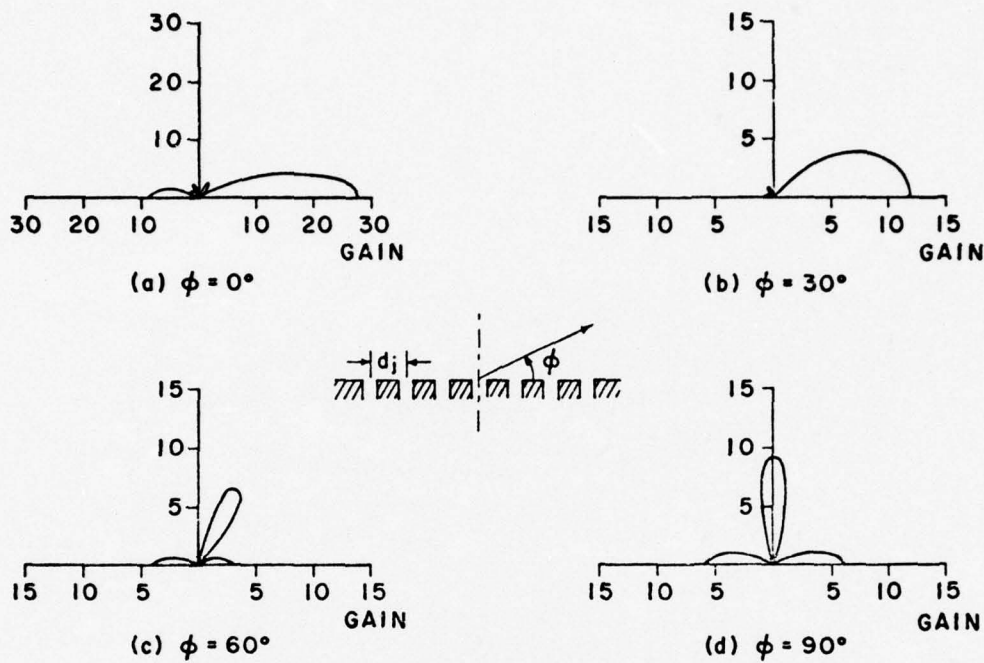


Fig. 12. Radiation gain patterns for a nine element reactively loaded aperture array when only the center aperture is externally driven, $d_j = 0.35\lambda$.

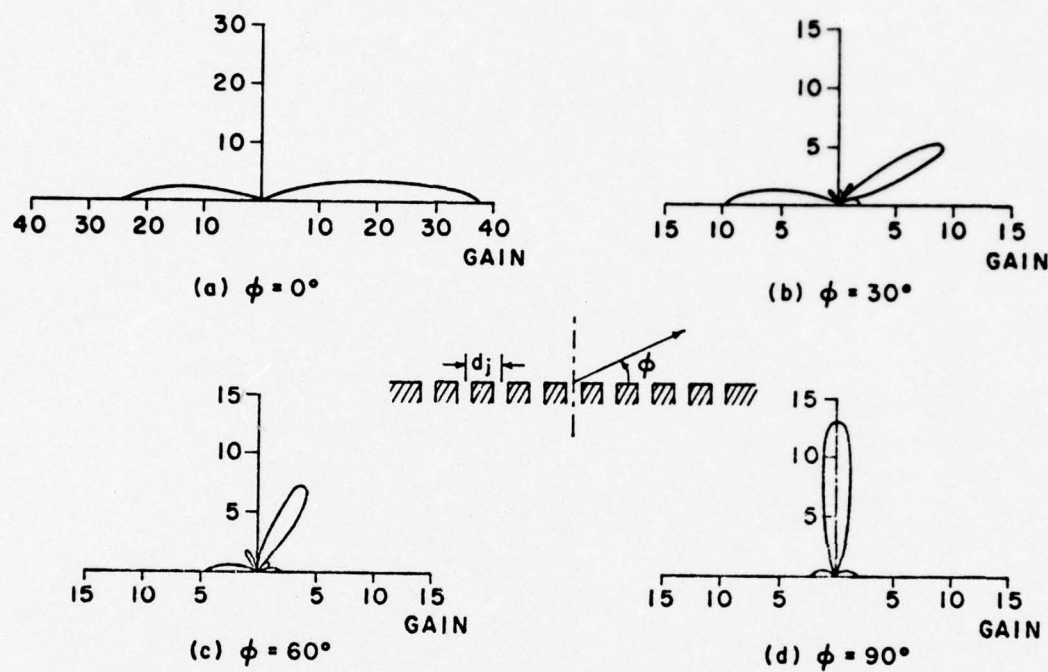


Fig. 13. Radiation gain patterns for a nine element reactively loaded aperture array when only the center aperture is externally driven, $d_j = 0.33\lambda$.

If it is desired to actively steer the antenna beam, the following technique is proposed. A waveguide to microstrip transition along with p-i-n diodes imbedded in a microstrip transmission line (see Fig. 14) is one possible realization for the variable reactive load.

Due to the increased availability of microstrip components using MIC technology, the use of waveguide to microstrip transistions has become more prevalent in the microwave industry. J. Heuven of the Philip's Research Laboratories [9] has fabricated a waveguide to microstrip transition that exhibits increased bandwidth due to the employment of a stepped ridge waveguide transformer. He claims that lower reflectivity than previous designs has been achieved. The waveguide to microstrip transition shown in Fig. 14 is a modification of his design.

To realize variable short circuits terminating a transmission line, the use of p-i-n diodes for the active shorting elements along with microstrip for the transmission line is proposed. Under zero and reverse bias, a p-i-n diode exhibits very high impedance at microwave frequencies, whereas at moderate forward currents it has a very low impedance. These characteristics permit the use of p-i-n diodes as the active electrical shorting element in the proposed design.

The entire circuit including waveguide to microstrip transition could be housed inside the reactive load waveguide. In addition, the waveguide would provide adequate rf shielding for the microstrip circuit.

For the lower frequency range and lower dielectric constants normally used for microstrip circuit fabrication, commercially available p-i-n diodes could be used in their cylindrical shaped package, while for the higher frequencies and dielectric constants, the p-i-n diode chip would have to be used. This leads to the feasibility of MIC circuit fabrication techniques which would provide a rather compact package for the entire reactive load. M. E. Davis [10] has clearly demonstrated that this fabrication technology is at hand.

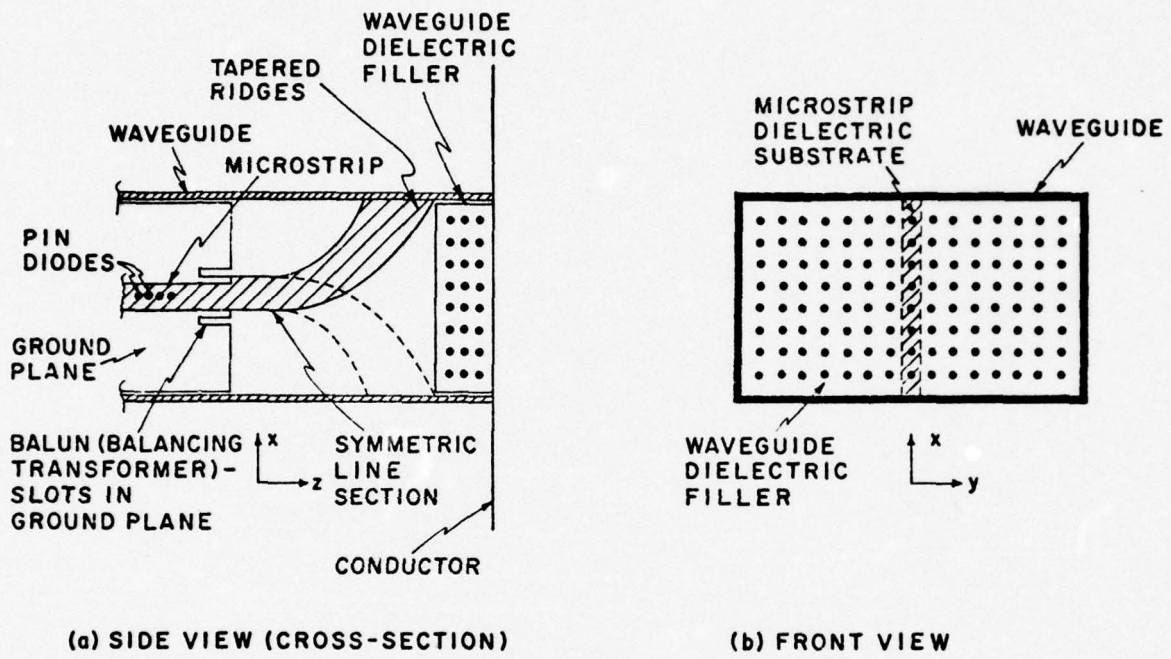


Fig. 14. Proposed design for a variable reactive load specified by equation (19).

VII. DISCUSSION AND CONCLUSIONS

The computer program has its basic limitations as does any mathematical model of a physical system. One limitation involves the spacing between apertures and the aperture width (some kind of failing as in a thin-wire dipole array problem). This limitation is most prevalent in the high Q operating region of the aperture array. Numerically, the matrix Real (Y^{HS}) used in the gain calculations is numerically not positive definite (see Table 1) and, therefore, the gain becomes unbounded. The high Q region of operation is usually not the most useful operating point. However, a lower Q region may yield an undesirable beamwidth at the lower beam steering angles. Therefore, an operating point in between appears to be the most promising.

While the gain is not a function of aperture width, the aperture admittance is related to it (see equation 22). Use of the thin dipole approximation for calculating the aperture admittances restricted us to using very narrow apertures. These small widths yielded aperture admittances and ultimately reactive load values (which are of the same order of magnitude) considerably less than the dominant mode wave admittance, Y_o . Tables 2 and 3 show the reactive load values required to obtain the data for the cases illustrated in Figs. 11 and 12. Y_o for these two cases is 1.97 mmho, which corresponds to a dielectric constant of $\epsilon_r = 1.55$. Therefore, due to the large difference in magnitudes between Y_o and the aperture admittances, a mismatch occurs at the waveguide aperture to half-space boundary. In addition, Tables 4 and 5 depict the short circuit distances required to realize the reactive loads given in Tables 2 and 3 for the $\phi = 0^\circ$ direction. The small distances required would make the physical realization suggested in the previous section difficult.

The analysis so far has considered only the lossless case. In reality, loss would be present in any physical realization. If loss were added, the thin dipole approximation would yield a positive definite half-space admittance matrix which would, in turn, allow greater aperture widths. Table 6 shows the $N=7$, $d_j = 0.27\lambda$ case considered in Table 4 but with 1% loss added. This allows a more reasonable aperture width of 0.1λ . Figure 15 illustrates the gain patterns in this lossy case (compare Fig. 11 with Fig. 15 to note the reduction in gain).

Table 1. Eigenvalues for Real (Y^{HS}) -- $N=7$, $d_j = 0.25\lambda$

APERTURE WIDTH				
EIGENVALUE				
No.	$W = 0.01\lambda$	$W = 0.02\lambda$	$W = 0.03\lambda$	$W = 0.04\lambda$
1	0.86×10^{-4}	0.17×10^{-3}	0.26×10^{-3}	0.34×10^{-3}
2	0.80×10^{-4}	0.16×10^{-3}	0.24×10^{-3}	0.32×10^{-3}
3	0.63×10^{-4}	0.13×10^{-3}	0.19×10^{-3}	0.25×10^{-3}
4	0.49×10^{-4}	0.98×10^{-4}	0.15×10^{-3}	0.20×10^{-3}
5	0.94×10^{-5}	0.19×10^{-4}	0.28×10^{-4}	0.38×10^{-3}
6	0.49×10^{-6}	0.98×10^{-6}	0.14×10^{-5}	0.19×10^{-5}
7	0.63×10^{-8}	0.22×10^{-9}	-0.31×10^{-7}	-0.10×10^{-6}

Table 2. Reactive load values (mmhos) for a seven element aperture array for $d_j = 0.27\lambda$ and $W = 0.01\lambda$ (see Fig. 11).

APERTURE NO.	$\phi = 0^\circ$	$\phi = 30^\circ$	$\phi = 60^\circ$	$\phi = 90^\circ$
1	-0.007 mΩ	-0.008 mΩ	-0.011 mΩ	-0.006 mΩ
2	-0.026	-0.029	-0.033	-0.033
3	-0.034	-0.037	-0.032	-0.032
5	-0.036	-0.032	-0.037	-0.032
6	-0.026	-0.030	-0.026	-0.033
7	-0.057	-0.027	-0.021	-0.006

Table 3. Reactive load values (mmhos) for a seven element aperture array for $d_j = 0.35\lambda$ and $W = 0.10\lambda$ (see Fig. 12).

APERTURE NO.	$\phi = 0^\circ$	$\phi = 30^\circ$	$\phi = 60^\circ$	$\phi = 90^\circ$
1	-0.121 mΩ	-26.4 mΩ	-0.235 mΩ	-0.083 mΩ
2	-0.342	-0.108	-1.36	-0.635
3	-0.442	-0.363	-0.191	-0.345
5	-0.507	-0.689	-0.858	-0.345
6	-0.466	-0.842	-0.227	-0.635
7	-0.284	-11.3	-0.333	-0.083

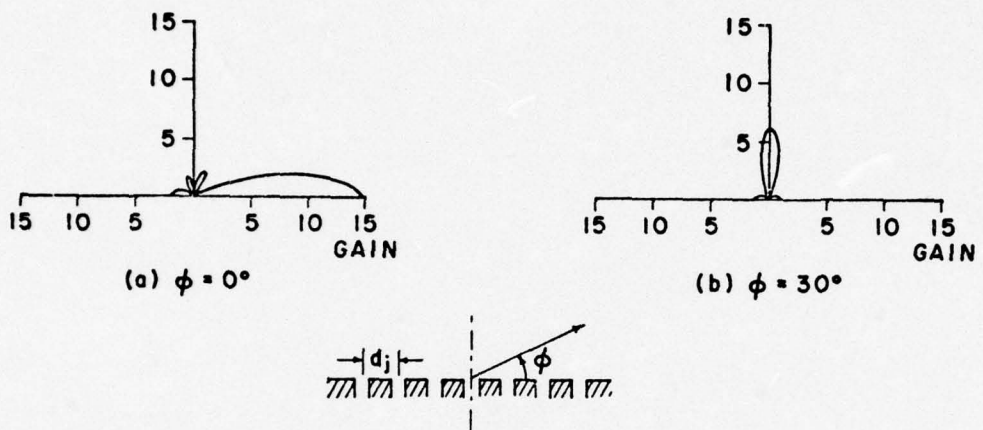


Fig. 15. Radiation gain patterns for a seven element reactively loaded aperture array when only the center element is externally driven, $d_j = 0.27\lambda$, and a loss of 1% is added.

Table 4. Short circuit distances for reactive load realization for $\phi = 0^\circ$, $d_j = 0.27\lambda$, $W = 0.01\lambda$, and freq. = 2.9 GHz.

APERTURE NO.	B_{Load}	$d^1(\phi) (\epsilon_r = 1.1)$	$d^1(\phi) (\epsilon_r = 1.55)$
1	-0.007 mV	81.4 mm	34.8 mm
2	-0.026	80.2	34.6
3	-0.034	79.7	34.5
5	-0.036	79.6	34.5
6	-0.026	80.2	34.6
7	-0.057	78.3	34.3

Table 5. Short circuit distances for reactive load realization for $\phi = 0^\circ$, $d_j = 0.35\lambda$, $W = 0.10\lambda$, and freq. = 2.9 GHz.

APERTURE NO.	B_{Load}	$d^1(\phi) (\epsilon_r = 1.1)$	$d^1(\phi) (\epsilon_r = 1.55)$
1	-0.121 mV	74.5 mm	33.5 mm
2	-0.342	61.7	31.1
3	-0.442	56.6	30.0
5	-0.507	53.5	29.3
6	-0.466	55.4	29.7
7	-0.284	64.8	31.7

Table 6. Short circuit distances for reactive load realization for $\phi = 0^\circ$, $d_j = 0.27\lambda$, $W = 0.10\lambda$, loss added = 1%, and freq. = 2.9 GHz.

APERTURE NO.	B_{Load}	$d^1(\phi) (\epsilon_r = 1.1)$	$d^1(\phi) (\epsilon_r = 1.55)$
1	-0.075 mV	77.2 mm	34.0 mm
2	-0.435	56.9	30.0
3	-2.622	16.1	14.3
5	-0.380	59.7	30.6
6	-0.372	60.1	30.7
7	-0.208	69.2	32.5

In this report, a fabrication technique is suggested for the physical realization of the reactive loads. In some respects, this reactive load realization might be considered more complex than a variable ferrite phase shifter and on equal par with switched delay line and p-i-n reactive diode phase shifters. However, reduction in the number of direct-fed elements in the reactive load case certainly is advantageous.

Work should be continued to minimize the 180° back lobe at the lower beam steering angles for higher N and higher Q-mode aperture arrays. Also, some attention should be given to a possible composite array using phase shifters and reactive loads. Phase shifters could be used for the major beam steering and variable reactive loads used to obtain other desirable properties such as minimizing unwanted sidelobes.

PART TWO
COMPUTER PROGRAMS

I. INTRODUCTION

A computer program used to generate the figures in this report along with a numerical example is presented in this part of the report. This program consists of the subroutines: YHSP, SICI, PATHSP, MAXGCV, MAXGRV, LINER, BLOADC, BLOADR, FUNCTA, FUNCTB, LINEQ, EIGEN, and the calling MAIN program. Each subroutine computes one function only and can be used or not used if that specific output is or is not required.

II. ADMITTANCE MATRIX

The subroutine YHSP (N, X, W, L, YHS) computes and stores columnwise in YHS, the elements of the admittance matrix.

$$\begin{aligned} Y_{ij}^{hs} = & \frac{1}{\eta\pi} \left(\frac{w}{L}\right) [2 Ci(kd) - Ci(u_2) - Ci(v_2)] \\ & - \frac{j}{\eta\pi} \left(\frac{w}{L}\right) [2 Si(kd) - Si(u_2) - Si(v_2)] \end{aligned} \quad (1)$$

where

$$u_2 = k (\sqrt{d^2 + L^2} + L)$$

$$v_2 = k (\sqrt{d^2 + L^2} - L) .$$

There are N apertures. X(I) is equal to kX_i where k is the propagation constant and X_i is the coordinate of the I-th aperture. w is the aperture length. The IJ-th element of the port admittance matrix is computed inside nested DO loops 10 and 11 and is stored in both $YHS(I + (J-1) * N)$ and $YHS(J + (I-1) * N)$.

Minimum allocations are given by

COMPLEX YHS (N*N)

DIMENSION X(N)

The subroutine SICI(SI,CI,X) stores the sine and cosine integrals

$$Ci(x) = - \int_x^{\infty} \frac{\cos v}{v} dv \quad (2)$$

$$Si(x) = \int_0^x \frac{\sin v}{v} dv \quad (3)$$

in SI and CI respective. SICI is the subroutine SICI in the IBM Scientific Subroutine Package * with SI replaced by $SI + \frac{\pi}{2}$.

*IBM/360 Scientific Subroutine Package (360A-CM-03x) Version III,
Programmer's Manual, page 370.

```

SUBROUTINE YHSP(N,X,W,L,YHS)
COMPLEX YHS(99),U
DIMENSION X(9)
REAL L,L1
PI=3.141593
ETA=376.730
L=L/2.
L1=L*2.*PI
T=2.
U=(0.,1.)
L2=L1*L1
TL=T*L1
TL2=TL*TL
CS=COS(L1)
SN=SIN(L1)
C1=W/(PI*ETA*L*SN*SN)
C2=SN*CS
C3=.5*COS(TL)
J2=0
DO 10 J=1,N
J1=J
DO 11 I=1,J
J3=J2+I
IF(I-J) 12,13,12
13 IF(I-1) 14,15,14
14 YHS(J1)=YHS(1)
GO TO 11
15 D=(W*2.*PI)/4.
D2=D*D
GO TO 16
12 XJ=X(I)-X(J)
D2=XJ*XJ
D=SQRT(D2)
16 S1=SQRT(D2+L2)
S2=SQRT(D2+TL2)
V1=S1+L1
U1=D2/V1
U2=S2+TL
V2=D2/U2
CALL SICI(SD,CD,D)
CALL SICI(SU1,CU1,U1)
CALL SICI(SV1,CV1,V1)
CALL SICI(SU2,CU2,U2)
CALL SICI(SV2,CV2,V2)
YHS1=C1*(C2*(SU2-SV2-T*(SV1-SU1))-C3*(T*(CU1-CD+CV1)-CU2-CV2)-CU1+
1T*CD-CV1)
YHS2=C1*(C2*(CV2-CU2+T*(CV1-CU1))-C3*(T*(SU1-SD+SV1)-SU2-SV2)-SU1+
1T*SD-SV1)
YHS(J1)=YHS1-U*YHS2
YHS(J3)=YHS(J1)
J1=J1+N
11 CONTINUE
J2=J2+N
10 CONTINUE
RETURN
END

```

```

SUBROUTINE SICI(SI,CI,X)
Z=ABS(X)
IF(Z>4.)1,1,4
1 Y=(4.-Z)*(4.+Z)
3 SI=X*(((((1.7531+1E-9*Y+1.568988E-7)*Y+1.374168E-5)*Y+6.939889E-4)
1*Y+1.964882E-2)*Y+4.395509E-1)
CI=((5.772156E-1+ALOG(Z))/Z-Z*(((((1.386985E-10*Y+1.584995E-6)*Y
1+1.725752E-6)*Y+1.185999E-4)*Y+4.990920E-3)*Y+1.315308E-11)/Z
RETURN
4 SI=SIN(Z)
Y=CES(Z)
Z=4./Z
U=((((((((4.048069E-3*Z-2.279143E-2)*Z+5.515070E-2)*Z-7.261642E-2)
1*Z+4.987716E-2)*Z-3.332519E-3)*Z-2.314617E-2)*Z-1.134958E-5)*Z
2+6.250011E-2)*Z+2.583989E-10
V=(((((((-5.108699E-3*Z+2.819179E-2)*Z-6.537283E-2)*Z
1+7.902034E-2)*Z-4.400416E-2)*Z-7.945556E-3)*Z+2.601293E-2)*Z
2-3.764000E-4)*Z-3.122418E-2)*Z-6.646441E-7)*Z+2.500000E-1
CI=Z*(SI*V-Y*U)
SI=-Z*(SI*U+Y*V)      +1.570796
RETURN
END

```

III. MEASUREMENT VECTOR, P^M

The subroutine PATHSP(N,X,L,W,PME,PMH) computes the E and H plane wave measurement vectors, PME and PMH where

$$PMH = \frac{4\sqrt{2}}{k} \sqrt{\frac{w}{L}} \frac{\cos(\frac{\pi}{2} \cos \theta)}{\sin \theta} \quad (5)$$

The output is stored in PME(N,J) and PMH(N,J) for $\phi = (J - 1) * \frac{\pi}{36}$,
 $J = 1, 2, \dots, 37$.

The input variables are the same as YHS.

Minimum allocations are given by

COMPLEX PME(N,37), PMH(N,37)

DIMENSION X(N)

```
SUBROUTINE PATHSP(N,X,L,W,PME,PMH)
COMPLEX PMH(9,37),PMF(9,37),S,S1,U
DIMENSION X(9)
REAL L,L1
PI=3.141593
U=(0.,1.)
L1=L*2.*PI
W1=W*PI
DELT=PI/36
C1=-4.*SQRT(2.*W/L)
C2=-1.*C1
DO 10 I=1,N
DO 11 J=1,37
PH=(J-1)*DELT
CS=CCS(PH)
SN=SIN(PH)
S=COS(X(I)*CS)+U*SIN(X(I)*CS)
IF(I.EQ.19) PMF(I,J)=C1*S
IF(I.EQ.19) GO TO 12
PME(I,J)=C1*S*SIN(W1*CS)/(W1*CS)
12 CONTINUE
IF(I.GT.1) PMH(I,J)=PMH(I,J)
IF(I.GT.1) GO TO 11
IF(J.EQ.1) PMH(I,J)=C2
IF(J.EQ.37) PMH(I,J)=C1
IF((J.EQ.1).OR.(J.EQ.37)) GO TO 11
S1=COS(PI*CS/2./I/SN
PMH(I,J)=C2*S1
11 CONTINUE
10 CONTINUE
RETURN
END
```

IV. MAXIMUM GAIN, COMPLEX AND REAL EQUIVALENT VOLTAGE SOURCES, ALL APERTURE FED

(The derivation of the formulas found in this section can be found in reference [11].)

The subroutine MAXGCV(N,PMER,YHS,VCMR) computes the maximum gain, GC, using complex equivalent voltage sources for excitation. These sources are outputted, VCMR, so that BLOADC can compute the reactive loads needed to resonate these sources for a starting point for the optimization program.

$$GC = \frac{k^2}{8\pi\eta} \tilde{P}^m [G^{hs}]^{-1} \tilde{P}^{m*} \quad (6)$$

$$VCMR = [G^{hs}]^{-1} \tilde{P}^{m*} \quad (7)$$

In the program, the constant $\frac{k^2}{8\pi\eta}$ has been changed to $\frac{1}{8\pi\eta}$ because the measurement vectors, \tilde{P}^m , have been multiplied by k to make them insensitive to absolute length.

The subroutine MAXGRV(N,PMER,YHS,VRMR) computes the maximum real gain, GR, restricting the array excitation to real or equiphasal equivalent voltage sources. These sources are outputted, VRMR, so that BLOADR can compute the reactive loads which resonate these sources.

$$GR = \frac{k^2}{8\pi\eta} \text{Real}(\tilde{P}^m) [G^{hs}]^{-1} \{\text{Real}(\tilde{P}^m) + c \text{Imag}(\tilde{P}^m)\} \quad (8)$$

$$VRMR = [G^{hs}]^{-1} [\text{Real}(\tilde{P}^m) + c \text{Imag}(\tilde{P}^m)] \quad (9)$$

where

$$c = -a \pm (a^2 + 1)^{1/2}$$

$$a = \frac{\text{Real}(\tilde{P}^m) [G^{hs}]^{-1} \text{Real}(\tilde{P}^m) - \text{Imag}(\tilde{P}^m) [G^{hs}]^{-1} \text{Imag}(\tilde{P}^m)}{2 \text{Real}(\tilde{P}^m) [G^{hs}]^{-1} \text{Imag}(\tilde{P}^m)}$$

Note: There are two possible real solutions for c which make GR stationary.
The maximum gain is obtained by using the larger of the two values.

Minimum allocations are given by

```
COMPLEX PMER(N), YHS(N*N)
DIMENSION G(N*N), V1(N),V2(N),A1(N),A2(N),VRMR(N)
```

The subroutine LINER(LL,C) is an inversion subroutine for real matrices.

Minimum allocations are given by

```
DIMENSION LR(N),C(N*N)
```

```

SUBROUTINE MAXGCV(N,PMER,YHS,VCMR)
COMPLEX CCNJC,GC1(9),PMER(9),VCMR(9),YHS(99)
DIMENSION G(99)
PI=3.141593
ETA=376.730
NN=N*N
C1=1./(8.*PI*ETA)
DO 1 J=1,NN
G(J)=REAL(YHS(J))
1 CONTINUE
CALL LINER(N,G)
DO 3 K=1,N
GC1(K)=(0.,0.)
VCMR(K)=(0.,0.)
3 CONTINUE
J1=1
DO 4 K=1,N
DO 5 J=1,N
GC1(K)=GC1(K)+PMER(J)*G(J1)
J1=J1+1
5 CONTINUE
4 CONTINUE
GC=0.
DO 6 K=1,N
GC=GC+REAL(GC1(K))*CONJG(PMER(K)))
6 CONTINUE
GC=GC*C1
J1=1
DO 7 K=1,N
DO 8 J=1,N
VCMR(K)=VCMR(K)+G(J1)*CONJG(PMER(J)))
J1=J1+N
8 CONTINUE
J1=K+1
7 CONTINUE
WRITE(3,10) GC
WRITE(3,11) (VCMR(J),J=1,N)
10 FORMAT(/3X,'COMPLEX GAIN =',1F5.2)
11 FORMAT(/1X,' COMPLEX EQUIVALENT VOLTAGE FOR MAXIMUM COMPLEX GAIN'
1//(3X,5E14.7))
RETURN
END

SUBROUTINE MAXGRV(N,PMER,YHS,VRMR)
COMPLEX PMER(9),YHS(99)
DIMENSION G(99),V1(9),V2(9),A1(9),A2(9),VRMR(9)
PI=3.141593
ETA=376.730
NN=N*N
C1=1./(8.*PI*ETA)
DO 1 J=1,NN
G(J)=REAL(YHS(J))
1 CONTINUE
CALL LINER(N,G)
DO 2 I=1,N
V1(I)=REAL(PMER(I))
V2(I)=AIMAG(PMER(I))
2 CONTINUE
DO 3 K=1,N

```

```

VRMR(K)=0.
A1(K)=0.
A2(K)=0.
J3=(K-1)*N
DO 4 I=1,N
J1=J3+I
A1(K)=A1(K)+G(J1)*V1(I)
A2(K)=A2(K)+G(J1)*V2(I)
4 CONTINUE
3 CONTINUE
S1=0.
S2=0.
S3=0.
DO 5 K=1,N
S1=S1+V1(K)*A1(K)
S2=S2+V2(K)*A2(K)
S3=S3+V1(K)*A2(K)
5 CONTINUE
S4=S1-S2
IF(S3.EQ.0.) S3=S4*1.E-14
A=S4/(2.*S3)
SA=SQRT(A*A+1.)
C=-A+SIGN(SA,S3)
GR=C1*(S1+C*S3)
WRITE(3,20) GP
20 FORMAT(1/3X,'MAXIMUM REAL GAIN =',1F5.2)
DO 9 I=1,N
VRMR(I)=A1(I)+C*A2(I)
9 CONTINUE
WRITE(3,21) (VRMR(I),I=1,N)
21 FORMAT(1/3X,'REAL EQUIVALENT VOLTAGE FOR MAXIMUM REAL GAIN'//(3X,5D
14.7))
RETURN
END

SUBROUTINE LINER(LL,C)
DIMENSION LR(30),C(99)
DO 20 I=1,LL
LR(I)=I
20 CONTINUE
M1=0
DO 18 M=1,LL
K=M
DO 2 I=M,LL
K1=M1+I
K2=M1+K
IF(ABS(C(K1))-ABS(C(K2))) 2,2,6
6 K=I
2 CONTINUE
LS=LR(M)
LR(M)=LR(K)
LR(K)=LS
K2=M1+K
STOP=C(K2)
J1=0
DO 7 J=1,LL
K1=J1+K

```

```
K2=J1+M
ST0=C(K1)
C(K1)=C(K2)
C(K2)=ST0/ST0R
J1=J1+LL
7 CONTINUE
K1=M1+M
C(K1)=1./ST0R
DO 11 I=1,LL
IF(I-M) 12,11,12
12 K1=M1+I
ST=C(K1)
C(K1)=0.
J1=0
DO 10 J=1,LL
K1=J1+I
K2=J1+M
C(K1)=C(K1)-C(K2)*ST
J1=J1+LL
10 CONTINUE
11 CONTINUE
M1=M1+LL
18 CONTINUE
J1=0
DO 9 J=1,LL
IF(J-LR(J)) 14,8,14
14 LRJ=LR(J)
J2=(LRJ-1)*LL
21 DO 13 I=1,LL
K2=J2+I
K1=J1+I
S=C(K2)
C(K2)=C(K1)
C(K1)=S
13 CONTINUE
LR(J)=LP(LRJ)
LP(LRJ)=LRJ
IF(J-LR(J)) 14,8,14
8 J1=J1+LL
9 CONTINUE
RETURN
END
```

V. RESONANT LOADS

The subroutine BLOADC(N,NFP,BLOAD,VCMR,YHS) stores in BLOAD, the reactive loads

$$BLOAD(I) = \frac{\text{Imag} \left[- \sum_{J=1, J \neq I}^N Y^{IJ} V_J \right] - \text{Real}(Y^{II}) * \text{Imag}(V_I)}{\text{Real}(V_I)} \quad (10)$$

for $I = 1, \dots, N$

which resonate the complex equivalent voltages VCMR. NFP is the aperture feed port number.

Minimum allocations are given by

```
COMPLEX VCMR(N), YHS(N*N)
DIMENSION BLOAD(N)
```

The subroutine BLOADR(N,NFP,BLOAD,VRMR,YHS) stores in BLOAD, the reactive loads

$$BLOAD(I) = \frac{-1}{V(I)} ([B^{hs}] * \vec{V})_I \quad (11)$$

(where $([B^{hs}] * \vec{V})_I$ denotes the I-th component of the column matrix $[B^{hs}] * \vec{V}$)

which resonates the real equivalent voltages, VRMR.

(Derivation of this formula can be found in reference [11].)

(Note that it can be easily shown that the gain does not depend on $BLOAD(I)$ where $I = \frac{k+1}{2}$ (driven aperture).)

Minimum allocations are given by

```
COMPLEX YHS(N*N)
DIMENSION BLOAD(N), VRMR(N)
```

```
SUBROUTINE BLOADC(N,NFP,BLOAD,VCMR,YHS)
COMPLEX U1,VCMR(9),YHS(99)
DIMENSION BLOAD(9)
J1=1
DO 1 I=1,N
J2=I
U1=(0.,0.)
DO 2 K=1,N
IF(K.EQ.I) GO TO 3
U1=U1-YHS(J2)*VCMR(K)
3 CONTINUE
J2=J2+N
2 CONTINUE
BLOAD(I)=(AIMAG(U1)-REAL(YHS(J1)))*AIMAG(VCMR(I))/REAL(VCMR(I))-AIMAG(YHS(J1))
J1=J1+N+1
1 CONTINUE
BLOAD(NFP)=0.
WRITE(3,4) (BLOAD(I),I=1,N)
4 FORMAT(/3X,'BLOAD-RESONATING COMPLEX SOURCES'/(3X,5E14.7))
RETURN
END

SUBROUTINE BLOADR(N,NFP,BLOAD,VRMR,YHS)
COMPLEX YHS(99)
DIMENSION BLOAD(9),VRMR(9)
DO 1 I=1,N
J1=I
U1=C.
DO 2 K=1,N
U1=U1+(AIMAG(YHS(J1)))*VRMR(K)
J1=J1+N
2 CONTINUE
BLOAD(I)=-U1/VRMR(I)
1 CONTINUE
BLOAD(NFP)=0.
WRITE(3,3) (BLOAD(I),I=1,N)
3 FORMAT(/3X,'BLOAD-RESONATING REAL SOURCES'/(3X,5E14.7))
RETURN
END
```

VI. GAIN PATTERNS

The subroutine FUNCTA(N,GAIN,PMER,V,YHS) computes the gain (all apertures excited) using the following equation

$$GAIN = \frac{k^2}{8\pi n \operatorname{Real}(\tilde{V}[Y^{hs}] * \tilde{V}^*))} |\tilde{P}^m \tilde{V}|^2 \quad (12)$$

for a given measurement vector PMER and excitation vector, \tilde{V} .

Minimum allocations are given by

COMPLEX PMER(N), V(N), V1(N), YHS(N*N).

The subroutine FUNCTB(N,NFP,BLOAD,GAIN,PMER,YHS) computes the gain using formula (12) with the following modification. The excitation is that of a unit current source for a single aperture (NFP) and the other apertures reactively loaded (BLOAD). Therefore,

$$V = [Y^{hs} + j BLOAD]^{-1} * \vec{I}(NFP) \quad (13)$$

where

$$\vec{I}(NFP) = \begin{bmatrix} 0 \\ \vdots \\ 1 \\ \vdots \\ 0 \end{bmatrix}$$

Minimum allocations are given by

COMPLEX PMER(N), V(N), V1(N), Y(N*N), YHS (N*N)
DIMENSION BLOAD(N), G(N*N) .

The subroutine LINEQ(LL,C) is used in FUNCTB to invert a complex matrix.

Minimum allocations are given by

COMPLEX C(N*N)
DIMENSION LR(N)

```

SUBROUTINE FUNCTA(N,GAIN,PMER,V,YHS)
COMPLEX CONJG,PMER(9),V(9),V1(9),V2,YHS(99)
ETA=376.730
PI=3.141593
C1=1./(8.*PI*ETA)
V2=(0.,0.)
DO 1 J=1,N
V1(J)=(0.,0.)
J3=(J-1)*N
DO 2 I=1,N
J4=J3+I
V1(J)=V1(J)+CONJG(YHS(J4))*CONJG(V(I))
2 CONTINUE
V2=V2+V1(J)*V(J)
1 CONTINUE
DEN=REAL(V2)
V2=(0.,0.)
DO 3 J=1,N
V2=V2+V(J)*PMER(J)
3 CONTINUE
GAIN=(C1*V2*CONJG(V2))/DEN
RETURN
END

SUBROUTINE FUNCTB(N,NFP,BLOAD,GAIN,PMER,YHS)
COMPLEX CONJG,PMER(9),U1,V(9),V1(9),V2,Y(99),YHS(99)
DIMENSION BLOAD(9),G(99)
ETA=376.730
PI=3.141593
C1=1./(8.*PI*ETA)
U1=(0.,1.)
NN=N*N
NL=N+1
DO 1 J=1,NN
Y(J)=YHS(J)
G(J)=REAL(YHS(J))
1 CONTINUE
J3=-N
DO 2 J=1,N
J3=J3+NL
Y(J3)=Y(J3)+U1*BLOAD(J)
2 CONTINUE
CALL LINEQ(N,Y)
I3=(NFP-1)*N
DO 3 J=1,N
I4=I3+J
V(J)=Y(I4)
3 CONTINUE
V2=(0.,0.)
DO 4 J=1,N
V1(J)=(0.,0.)
J3=(J-1)*N
DO 5 I=1,N
J4=J3+I
V1(J)=V1(J)+G(J4)*V(I)
5 CONTINUE
V2=V2+V1(J)*CONJG(V(J))

```

```

4 CONTINUE
DEN=REAL(V2)
V2=(0.,0.)
DO 7 J=1,N
V2=V2+V(J)*PMER(J)
7 CONTINUE
GAIN=(C1*REAL(V2*CONJG(V2)))/DEN
RETURN
END

SUBROUTINE LINEQ(LL,C)
COMPLEX C(99),STOR,ST0,ST,S
DIMENSION LR(58)
DO 20 I=1,LL
LR(I)=I
20 CONTINUE
M1=C
DO 18 M=1,LL
K=M
K2=M1+K
S1=ABS(REAL(C(K2)))+ABS(AIMAG(C(K2)))
DO 2 I=M,LL
K1=M1+I
S2=ABS(REAL(C(K1)))+ABS(AIMAG(C(K1)))
IF(S2-S1) 2,2,6
6 K=I
S1=S2
2 CONTINUE
LS=LR(M)
LR(M)=LR(K)
LR(K)=LS
K2=M1+K
STOR=C(K2)
J1=0
DO 7 J=1,LL
K1=J1+K
K2=J1+M
ST0=C(K1)
C(K1)=C(K2)
C(K2)=ST0/STOR
J1=J1+LL
7 CONTINUE
K1=M1+M
C(K1)=1./STOR
DO 11 I=1,LL
IF(I-M) 12,11,12
12 K1=M1+I
ST=C(K1)
C(K1)=0.
J1=0
DO 10 J=1,LL
K1=J1+I
K2=J1+M
C(K1)=C(K1)-C(K2)*ST
J1=J1+LL
10 CONTINUE
11 CONTINUE
M1=M1+LL
18 CONTINUE
J1=0
DO 9 J=1,LL

```

```
IF(J-LR(J)) 14,8,14
14 LRJ=LR(J)
      J2=(LRJ-1)*LL
21 DC 13 I=1,LL
      K2=J2+I
      K1=J1+I
      S=C(K2)
      C(K2)=C(K1)
      C(K1)=S
13 CONTINUE
      LR(J)=LR(LRJ)
      LR(LRJ)=LRJ
      IF(J-LR(J)) 14,8,14
8   J1=J1+LL
9   CONTINUE
      RETURN
      END
```

VII. EIGENVALUE DETERMINATION

The subroutine EIGEN(A,R,N,MV) is used to determine whether $G = \text{Real}(Y^{\text{hs}})$ is a positive definite matrix. This subroutine is taken from IBM Scientific Subroutine Package*. It can only be used for real symmetric matrices.

MV should be set equal to 1 (done in the main program) for eigenvalues only. The original matrix A must be stored in upper triangular form and the eigenvalues are outputted on the diagonal of A (therefore, the input matrix, A, is wiped-out during execution of the subroutine).

Minimum allocations (for eigenvalue determination only) are given by

DIMENSION A(N*N/2), R(1)

*IBM/360 Scientific Subroutine Package (360A-CM-03X), Version III,
Programmer's Manual, pages 164-165.

```

SUBROUTINE EIGEN(A,R,N,MV)
DIMENSION A(144),R(144)
IF(MV-1) 10,25,10
10 IQ=-N
DO 20 J=1,N
IQ=IQ+N
DO 20 I=1,N
IJ=IQ+I
R(IJ)=0.0
IF(I-J) 20,15,20
15 R(IJ)=1.0
20 CONTINUE
25 ANORM=0.0
DO 35 I=1,N
DO 35 J=I,N
IF(I-J) 30,35,30
30 IA=I+(J*J-J)/2
ANORM=ANORM+A(IA)*A(IA)
35 CONTINUE
IF(ANORM) 165,165,40
40 ANORM=1.414*SQRT(ANORM)
ANRMX=ANORM*1.0E-6/FLOAT(N)
IND=0
THR=ANORM
45 THR=THR/FLOAT(N)
50 L=1
55 M=L+1
60 MQ=(M*M-M)/2
LQ=(L*L-L)/2
LM=L+MQ
62 IF(ABS(A(LM))-THR) 130,65,65
65 IND=1
LL=L+LQ
MM=M+MQ
X=0.5*(A(LL)-A(MM))
68 Y=-A(LM)/SQRT(A(LM)*A(LM)+X*X)
IF(X) 70,75,75
70 Y=-Y
75 SINX=Y/SQRT(2.0*(1.0+(SQRT(1.0-Y*Y))))
SINX2=SINX*SINX
78 COSX=SQRT(1.0-SINX2)
COSX2=COSX*COSX
SINCOS=SINX*COSX
ILQ=N*(L-1)
IMQ=N*(M-1)
DO 125 I=1,N
IQ=(I*I-I)/2
IF(I-L) 80,115,80
80 IF(I-M) 85,115,90
85 IM=I+MQ
GO TO 95
90 IM=M+IQ
95 IF(I-L) 100,105,105
100 IL=I+LQ
GO TO 110
105 IL=L+IQ
110 X=A(IL)*COSX-A(IM)*SINX

```

```

A(IM)=A(IL)*SINX+A(IM)*COSX
A(IL)=X
115 IF(MV-1) 120,125,120
120 ILR=ILQ+I
IMR=IMQ+I
X=R(ILR)*COSX-R(IMR)*SINX
R(IMR)=R(ILR)*SINX+R(IMR)*COSX
R(ILR)=X
125 CONTINUE
X=2.0*A(LM)*SINC
Y=A(LL)*COSX2+A(MM)*SINX2-X
X=A(LL)*SINX2+A(MM)*COSX2+X
A(LM)=(A(LL)-A(MM))*SINC+A(LM)*(COSX2-SINX2)
A(LL)=Y
A(MM)=X
130 IF(M-N) 135,140,135
135 M=M+1
GO TO 60
140 IF(L-(N-1)) 145,150,145
145 L=L+1
GO TO 55
150 IF(IND-1) 160,155,160
155 IND=0
GO TO 50
160 IF(THR-ANRMX) 165,165,45
165 IQ=-N
DO 185 I=1,N
IQ=IQ+N
LL=I+(I*I-I)/2
JQ=N*(I-2)
DO 185 J=I,N
JQ=JQ+N
MM=J+(J*J-J)/2
IF(A(LL)-A(MM)) 170,185,185
170 X=A(LL)
A(LL)=A(MM)
A(MM)=X
IF(MV-1) 175,185,175
175 DO 180 K=1,N
ILR=IQ+K
IMR=JQ+K
X=R(ILR)
R(ILR)=R(IMR)
180 R(IMR)=X
185 CONTINUE
RETURN
END

```

VIII. MAIN PROGRAM AND SAMPLE INPUT-OUTPUT DATA

The preceding six sections have described all of the necessary subroutines (except the optimization program) to generate the graphs contained in this report and other output data not included. The missing optimization subroutine is included in reference [1]. This subroutine is a univariate optimization program which was found to be very efficient (minimum CPU time) for optimizing the ratio of quadratic functions normally encountered in reactively loaded arrays (see reference [12]). The CALL statement for this optimization subroutine in the MAIN program (following 8 CONTINUE) reads

```
CALL MAXU(N,NFP,N9,STEP,BLOAD,PMER,YHS).
```

All of the calling arguments have been defined previously except N9 and STEP. N9 equals the number of complete searches (one search per revised load value) and STEP is related to the size of the incremental change in the load during the searching part of the program. Different STEP values should be tried. Too small a step will require more searches for a given relative maximum while too large a step might cause a maximum to be skipped past. One can use other optimization subroutines. The output should yield the optimum loads for maximizing the gain corresponding to a given measurement vector \vec{P}^m (direction).

The purpose of the MAIN program is to obtain input data and call subroutines to generate output data. Input data is read into the MAIN program according to

```
READ (1,201) N,W,L,NFP,NA,N9,STEP  
201 FORMAT (I2, 2F5.2, 2I2, 1I3, 1E9.2)  
      READ (1,214) (ANGLE(I),I=1,NA)  
214 FORMAT (10I3)  
      READ (1,216) ER  
216 FORMAT (1F7.2)  
      READ (1,216) L3
```

There are N apertures w-wide and L-long (L is assumed to be one-half wavelength). The x-coordinate of the I-th aperture is X(I). The feed aperture number is NFP. All of these arguments have been described previously with the exception of NA,ANGLE,ER, and L3. NA is the number of angles for which the gain will be optimized. This integer should correspond to the number of angles read in to form the array ANGLE(I). ER is the relative dielectric constant of the dielectric filler for the waveguide. This number can and probably would be different than the microstrip substrate dielectric proposed for the reactive loads. L3 is the length of the waveguide used in the calculation of the short positions from the optimum reactive load values.

Minimum allocations are given by

```
COMPLEX PMH(N,37),PME(N,37),PMER(N),YHS(N*N),V(N),VCMR(N)
DIMENSION A(N*N/2),ANGLE(37),BL1(N),BLOAD(N),G1(37),G2(37),
         G3(37),G4(37),NP(N),R(1),SHORT(N),VRMR(N),X(N)
```

DO loop 1 puts kx in x. DO loop 2 calculates the eigenvalues of Real (Y^{hs}) and will stop the program if any of these values are negative. DO loop 13 calculates the short positions (formula 19 in Part I) for the optimum reactive loads.

The sample input is for an eight element aperture array with feed element aperture number 4 and aperture spacing 0.29λ . The gain is optimized in the $\phi = 50^\circ$ direction. Loads which resonate real equivalent sources were used for initial starting points for the optimization program. (Note loads which resonate complex equivalent sources could have been used by changing the CALL BLOADR() statement to CALL BLOADC().) The MAXU optimization subroutine went through six complete searches for each aperture load value. Output gain values are given in 5° steps starting at 0° for the following four conditions.

- 1) Maximum Gain -- Complex equivalent voltage sources
- 2) Maximum Gain -- Real equivalent voltage sources
- 3) Maximum Gain -- Using reactive loads which resonate real equivalent voltage sources
- 4) Maximum Gain -- Using the optimum reactive loads.

C MAIN PROGRAM

```

COMPLEX PMH(9,37),PME(9,37),PMER(9),YHS(99)
COMPLEX V(9),VCMR(9)
DIMENSION A(144),ANGLE(37),BL1(9),BLOAD(9),G1(37),G2(37),G3(37)
DIMENSION G4(37),NP(9),R(144),SHORT(9),VRMR(9),X(9)
REAL L,L2,L3
INTEGER ANGLE
200 FORMAT(/3X,'N',6X,'W',7X,'L',4X,'NFP',4X,'NA',6X,'N9',7X,'STEP')
201 FORMAT(12,2F5.2,2I2,1I3,1E9.2)
202 FORMAT(/2X,I2,3X,1F5.2,3X,1F5.2,3X,I2,5X,I2,5X,I3,4X,1E9.2)
203 FORMAT(9F5.2)
204 FORMAT(/3X,'X',//(3X,9F5.2))
205 FORMAT(/2X,' Y--HALF SPACE'/(3X,5E14.7))
207 FORMAT(/3X,'APERTURE --',I2,6X,'PM = ',2E14.7)
208 FORMAT(/2X,' P -- MEASUREMENT VECTOR -- E-PLANE'//)
210 FORMAT(/3X,'MAXIMUM GAIN--COMPLEX EQUIVALENT VOLTAGE--EQUIVALENT C
1OMPLEX VOLTAGE FOR MAXIMUM GAIN --',3X,I3,' DEGREES'//)
211 FORMAT(/1X,' MAXIMUM GAIN --REAL EQUIVALENT VOLTAGE --EQUIVALENT
1REAL VOLTAGE FOR MAXIMUM GAIN --',3X,I3,' DEGREES'//)
213 FORMAT(/1X,' LOADS--BLOADS = ',I3,' DEGREES'//)
214 FORMAT(10I3)
215 FORMAT(/3X,'PATTERN ANGLES'//(3X,I13,' DEGREES'//))
216 FORMAT(1F7.2)
217 FORMAT(/3X,'RELATIVE PERMITTIVITY OF DIELECTRIC USED IN WAVEGUIDE
ELEMENTS = ',1F5.2)
218 FORMAT(/3X,'DISTANCES OF SHORTS FOR WAVEGUIDE LOADS = ',I3,' DEGRE
1ES'//)
219 FORMAT(/1X,'E-PLANE'//)
220 FORMAT(/3X,'GAIN PATTERNS --',3X,I3,' DEGREES'//)
221 FORMAT(/3X,'MAXIMUM GAIN - COMPLEX EQUIVALENT VOLTAGE'//(3X,7F7.2)
1)
222 FORMAT(/3X,'MAXIMUM GAIN - REAL EQUIVALENT VOLTAGE'//(3X,7F7.2))
223 FORMAT(/3X,'GAIN - LOADED APERTURES - MODAL RESONANCE LOADS'//(3X,
17F7.2))
224 FORMAT(/3X,'GAIN - LOADED APERTURES - OPTIMUM LOADS'//(3X,7F7.2))
225 FORMAT(/3X,'SHORT(',I1,') = ',1F6.3,' MM')
226 FORMAT(/3X,'EIGENVALUE ',I2,' = ',1E14.7)
227 FORMAT(/3X,'LENGTH OF APERTURE = ',1F6.2,' MM')

WRITE(3,200)
READ(1,201) N,W,L,NFP,NA,N9,STEP
WRITE(3,202) N,W,L,NFP,NA,N9,STEP
READ(1,214) (ANGLE(I),I=1,NA)
WRITE(3,215) (ANGLE(I),I=1,NA)
READ(1,216) ER
WRITE(3,217) ER
READ(1,216) L3
WRITE(3,227) L3
MV=1
PI=3.141593
PI2=2.*PI
ETA=376.730
NN=N*N
N1=N-1
READ(1,203) (X(I),I=1,N)
WRITE(3,204) (X(I),I=1,N)
DO 1 I=1,N
X(I)=X(I)*PI2

```

```

1 CONTINUE
L2=L
CALL YHSP(N,X,W,L2,YHS)
WRITE(3,205) (YHS(J),J=1,N)
C POSITIVE DEFINITE TEST FOR CONDUCTANCE MATRIX
JA=0
DO 2 J=1,N
JG=(J-1)*N
DO 3 I=1,J
JA=JA+1
JG=JG+1
A(JA)=REAL(YHS(JG))
3 CONTINUE
2 CONTINUE
CALL EIGEN(A,R,N,MV)
J2=1
DO 4 I=1,N
WRITE(3,226) I,A(J2)
IF(A(J2).LT.0.) GO TO 5
J2=J2+I+1
4 CONTINUE
CALL PATHSP(N,X,L,W,PME,PMH)
DO 6 I1=1,NA
I=((ANGLE(I1)*36)/180+1)
J1=ANGLE(I1)
WRITE(3,208)
DO 7 J=1,N
PMER(J)=PME(J,I)
WRITE(3,207) J,PMER(J)
7 CONTINUE
WRITE(3,219)
WRITE(3,210) J1
CALL MAXGCV(N,PMER,YHS,VCMR)
WRITE(3,211) J1
CALL MAXGRV(N,PMER,YHS,VRMR)
WRITE(3,213) J1
CALL BLOADR(N,NFP,BLOAD,VRMR,YHS)
DO 8 J=1,N
BL1(J)=BLOAD(J)
8 CONTINUE
CALL MAXU(N,NFP,N9,STEP,BLOAD,PMER,YHS)
DO 9 K=1,N
V(K)=(1.,0.)*VRMR(K)
9 CONTINUE
WRITE(3,220) J1
DO 10 M=1,37
DO 11 J=1,N
PMER(J)=PME(J,M)
11 CONTINUE
CALL FUNCTA(N,GAIN,PMER,VCMR,YHS)
G1(M)=GAIN
CALL FUNCTA(N,GAIN,PMER,V,YHS)
G2(M)=GAIN
CALL FUNCTB(N,NFP,BL1,GAIN,PMER,YHS)
G3(M)=GAIN
CALL FUNCTB(N,NFP,BLOAD,GAIN,PMER,YHS)
G4(M)=GAIN
10 CONTINUE

```

```

      WRITE(3,221) (G1(M),M=1,37)
      WRITE(3,222) (G2(M),M=1,37)
      WRITE(3,223) (G3(M),M=1,37)
      WRITE(3,224) (G4(M),M=1,37)
      I2=1
      DO 12 I=1,N1
      IF(I.EQ.NFP) I2=I2+1
      NP(I)=I2
      I2=I2+1
12 CONTINUE
      WRITE(3,218) J1
      DO 13 J=1,N1
      J2=NP(J)
      SHCRT(J2)=ATAN(SQRT(ER-1.)/(-BLOAD(J2)*ETA))/((P1*SQRT(ER-1.))/LB)
      WRITE(3,225) J2,SHCRT(J2)
13 CONTINUE
6 CONTINUE
5 CONTINUE
STOP
END

```

\$DATA

N	W	L	NFP	NA	N9	STEP
8	0.01	0.50	4	1	49	0.10E-06

PATTERN ANGLES

50 DEGREES

RELATIVE PERMITTIVITY OF DIELECTRIC USED IN WAVEGUIDE ELEMENTS = 1.05

LENGTH OF APERTURE = 51.72 MM

X

-1.16-0.87-0.58-0.29 0.00 0.29 0.58 0.87

Y--HALF SPACE

0.4119083E-04 0.2343455E-04 0.1780118E-04-0.1885384E-04-0.1233211E-04
-0.1068729E-04-0.6214996E-05 0.9807113E-05 0.8328394E-05 0.3244617E-05
0.1132107E-05-0.7153654E-05-0.6064485E-05 0.4198154E-06 0.1557118E-05
0.4996528E-05 0.1780118E-04-0.1885384E-04 0.4119083E-04 0.2343455E-04
0.1780114E-04-0.1885384E-04-0.1233213E-04-0.1068726E-04-0.6214984E-05
0.9807145E-05 0.8328398E-05 0.3244617E-05 0.1132104E-05-0.7153654E-05
-0.6064482E-05 0.4198476E-06-0.1233211E-04-0.1068729E-04 0.1780114E-04
-0.1885384E-04 0.4119083E-04 0.2343455E-04 0.1780118E-04-0.1885384E-04
-0.1233211E-04-0.1068729E-04-0.6214996E-05 0.9807113E-05 0.8328394E-05
0.3244617E-05 0.1132104E-05-0.7153654E-05-0.6214996E-05 0.9807113E-05
-0.1233213E-04-0.1068726E-04 0.1780118E-04-0.1885384E-04 0.4119083E-04
0.2343455E-04 0.1780118E-04-0.1885384E-04-0.1233211E-04-0.1068729E-04
-0.6214996E-05 0.9807113E-05 0.8328398E-05 0.3244617E-05 0.8328394E-05
0.3244617E-05-0.6214984E-05 0.9807145E-05-0.1233211E-04-0.1068729E-04
0.1780118E-04-0.1885384E-04 0.4119083E-04 0.2343455E-04 0.1780118E-04
-0.1885384E-04-0.1233211E-04-0.1068729E-04-0.6214984E-05 0.9807145E-05
0.1132107E-05-0.7153654E-05 0.8328398E-05 0.3244617E-05-0.6214996E-05
0.9807113E-05-0.1233211E-04-0.1068729E-04 0.1780118E-04-0.1885384E-04

0.4119083E-04 0.2343455E-04 0.1780118E-04-0.1885384E-04-0.1233213E-04
-0.1068726E-04-0.6064485E-05 0.4198154E-06 0.1132104E-05-0.7153654E-05
0.8328394E-05 0.3244617E-05-0.6214996E-05 0.9807113E-05-0.1233211E-04
-0.1068729E-04 0.1780118E-04-0.1885384E-04 0.4119083E-04 0.2343455E-04
0.1780114E-04-0.1885384E-04 0.1557118E-05 0.4996528E-05-0.6064482E-05
0.4198476E-06 0.1132104E-05-0.7153654E-05 0.8328398E-05 0.3244617E-05
-0.6214984E-05 0.9807145E-05-0.1233213E-04-0.1068726E-04 0.1780114E-04
-0.1885384E-04 0.4119083E-04 0.2343455E-04

EIGENVALUE 1 = 0.7963572E-04

EIGENVALUE 2 = 0.7481415E-04

EIGENVALUE 3 = 0.5902007E-04

EIGENVALUE 4 = 0.5514034E-04

EIGENVALUE 5 = 0.4829286E-04

EIGENVALUE 6 = 0.1181671E-04

EIGENVALUE 7 = 0.7898826E-06

EIGENVALUE 8 = 0.1440352E-07

P -- MEASUREMENT VECTOR -- E-PLANE

APERTURE -- 1 PM = 0.2194397E-01-0.7996443E 00

APERTURE -- 2 PM = 0.7451952E 00-0.2908552E 00

APERTURE -- 3 PM = 0.5578344E 00 0.5733526E 00

APERTURE -- 4 PM = -0.3111879E 00 0.7369359E 00

APERTURE -- 5 PM = -0.7999454E 00 0.0000000E 00

APERTURE -- 6 PM = -0.3111879E 00-0.7369359E 00

APERTURE -- 7 PM = 0.5578344E 00-0.5733526E 00

APERTURE -- 8 PM = 0.7451952E 00 0.2908552E 00

E-PLANE

COMPLEX GAIN = 10.24

COMPLEX EQUIVALENT VOLTAGE FOR MAXIMUM COMPLEX GAIN

-0.5144069E 05 0.5518969E 05 0.1294318E 06-0.1085418E 06-0.1723520E 06
0.1935308E 06 0.1972770E 06-0.2837579E 06-0.1845980E 06 0.2921681E 06
0.1111990E 06-0.2341103E 06-0.4962431E 05 0.1614949E 06 0.3082638E 05
-0.6887394E 05

MAXIMUM REAL GAIN = 5.75

REAL EQUIVALENT VOLTAGE FOR MAXIMUM REAL GAIN

-0.1347424E 06 0.2932548E 06-0.4644418E 06 0.6255159E 06-0.6255364E 06
0.4645058E 06-0.2933556E 06 0.1347722E 06

LOADS--BLOADS - 50 DEGREES

BLOAD-RESONATING REAL SOURCES

-0.1774331E-04-0.3073009E-04-0.3755363E-04 0.0000000E 00-0.3732933E-04
-0.3755678E-04-0.3073015E-04-0.1774960E-04

H1 = 0.1409969E 03 0.0000000E 00

H2 =-0.2527136E 06-0.1904715E 07

H3 =-0.2527211E 06 0.1904705E 07

H4 = 0.1545716E 12-0.3395200E 05

H5 = 0.1119568E 09

H6 =-0.1417972E 05

H7 = 0.2964023E 03

H8 = 0.3423529E 06

H9 =-0.1170265E 05

U1 =-0.1116607E 05 0.2477063E 04

DEN = 0.1349388E 03

GAIN = 2.32

MINIMIZATION OF Y=F(X) WITH RESPECT TO 1TH LOAD

X(1) = 0.5635927E 05

Y(1) = 0.4316356E 00

SZ = 0.1769241E 05

PRELIMINARY SEARCH ON THE NEGATIVE SIDE

0.5635927E 05 0.5635927E 05 0.5635927E 05 0.5635922E 05 0.5635915E 05

0.5635899E 05 0.5635871E 05 0.5635816E 05 0.5635700E 05 0.5635459E 05

0.5635012E 05

0.4316356E 00 0.4316353E 00 0.4316353E 00 0.4316357E 00 0.4316363E 00

0.4316371E 00 0.4316385E 00 0.4316417E 00 0.4316483E 00 0.4316612E 00

0.4316873E 00

PRELIMINARY SEARCH ON THE POSITIVE SIDE

60

0.5635927E 05 0.5635012E 05 0.5635931E 05 0.5635931E 05 0.5635935E 05
0.5635945E 05 0.5635959E 05 0.5635987E 05 0.5636042E 05 0.5636158E 05
0.5636389E 05 0.5636847E 05
0.4316356E 00 0.4316873E 00 0.4316353E 00 0.4316353E 00 0.4316348E 00
0.4316343E 00 0.4316335E 00 0.4316320E 00 0.4316289E 00 0.4316222E 00
0.4316092E 00 0.4315833E 00

FINAL SEARCH

0.5635927E 05 0.5636847E 05 0.5637767E 05 0.5639609E 05 0.5643290E 05
0.5650673E 05 0.5665497E 05 0.5695379E 05 0.5756094E 05 0.5881497E 05
0.6149443E 05 0.6765913E 05 0.8462663E 05 0.1697819E 06 0.1129528E 06
0.7519763E 05 0.9675919E 05 0.7963400E 05 0.9028719E 05 0.8736551E 05
0.9341119E 05 0.8880219E 05 0.8953856E 05 0.8916888E 05 0.8991131E 05
0.8935331E 05 0.8972456E 05 0.8944581E 05 0.8949219E 05 0.8939956E 05
0.8946900E 05 0.8942275E 05 0.8943431E 05 0.8941119E 05 0.8942856E 05
0.8941700E 05 0.8942563E 05 0.8942419E 05 0.8942713E 05 0.8942494E 05
0.8942638E 05 0.8942531E 05 0.8942606E 05 0.8942550E 05 0.8942588E 05
0.8942556E 05 0.8942575E 05 0.8942563E 05 0.8942563E 05
0.4316356E 00 0.4315833E 00 0.4315315E 00 0.4314275E 00 0.4312208E 00
0.4308078E 00 0.4299879E 00 0.4283701E 00 0.4252247E 00 0.4192838E 00
0.4087559E 00 0.3927505E 00 0.3783332E 00 0.4031472E 00 0.3831652E 00
0.3828393E 00 0.3786221E 00 0.3799509E 00 0.3779136E 00 0.3779763E 00
0.3781313E 00 0.3779101E 00 0.3779028E 00 0.3779041E 00 0.3779063E 00
0.3779030E 00 0.3779041E 00 0.3779027E 00 0.3779028E 00 0.3779028E 00
0.3779030E 00 0.3779027E 00 0.3779030E 00 0.3779030E 00 0.3779029E 00
0.3779030E 00 0.3779026E 00 0.3779030E 00 0.3779028E 00 0.3779027E 00
0.3779030E 00 0.3779029E 00 0.3779032E 00 0.3779029E 00 0.3779030E 00
0.3779030E 00 0.3779031E 00 0.3779026E 00 0.3779026E 00

MINIMIZATION OF Y=F(X) WITH RESPECT TO 2TH LOAD

X(1) = 0.3254139E 05
Y(1) = 0.3778771E 00
SZ = 0.1412473E 05

MINIMIZATION OF Y=F(X) WITH RESPECT TO 3TH LOAD

X(1) = 0.2662858E 05
Y(1) = 0.2656897E 00
SZ = 0.1385878E 05

MINIMIZATION OF Y=F(X) WITH RESPECT TO 5TH LOAD

X(1) = 0.2678859E 05
Y(1) = 0.2624720E 00
SZ = 0.1539332E 05

MINIMIZATION OF Y=F(X) WITH RESPECT TO 6TH LOAD

X(1) = 0.2662635E 05
Y(1) = 0.2388443E 00
SZ = 0.1769593E 05

MINIMIZATION OF Y=F(X) WITH RESPECT TO 7TH LOAD

X(1) = 0.3254133E 05
Y(1) = 0.2364689E 00
SZ = 0.1843652E 05

MINIMIZATION OF Y=F(X) WITH RESPECT TO 8TH LOAD

X(1) = 0.5633930E 05
Y(1) = 0.2125733E 00
SZ = 0.1759652E 05

FINAL VALUE OF GAIN = 4.96

FINAL VALUE OF GAIN = 5.89

FINAL VALUE OF GAIN = 6.32

FINAL VALUE OF GAIN = 6.41

FINAL VALUE OF GAIN = 6.47

FINAL VALUE OF GAIN = 6.53

FINAL VALUE OF GAIN = 6.58

FINAL REACTIVE LOAD VALUES

-0.1592384E-04-0.3593648E-04-0.3004982E-04 0.0000000E 00-0.4219809E-04

-0.3708874E-04-0.2924007E-04-0.3079978E-04

FINAL VALUE OF GAIN = 6.58

GAIN PATTERNS - - 50 DEGREES

MAXIMUM GAIN - COMPLEX EQUIVALENT VOLTAGE

0.58	0.58	0.54	0.41	0.17	0.00	0.34
1.81	4.65	8.06	10.24	9.54	6.12	2.20
0.15	0.24	0.83	0.66	0.12	0.05	0.35
0.38	0.11	0.01	0.18	0.29	0.16	0.01
0.07	0.26	0.29	0.13	0.00	0.18	0.67
1.20	1.43					

MAXIMUM GAIN - REAL EQUIVALENT VOLTAGE

0.08	0.05	0.00	0.02	0.08	0.06	0.00
0.31	1.58	3.78	5.75	5.86	3.75	1.10
0.00	0.54	1.00	0.47	0.00	0.47	1.00
0.54	0.03	1.10	3.75	5.86	5.75	3.78
1.58	0.31	0.00	0.06	0.08	0.02	0.00
0.05	0.08					

GAIN - LOADED APERTURES - MODAL RESONANCE LOADS

0.96	0.92	1.01	1.58	2.56	3.26	2.84
1.37	0.11	0.48	2.32	3.70	3.06	1.20
0.56	1.29	1.66	0.74	0.00	0.69	1.62
1.32	0.67	1.45	3.25	3.87	2.44	0.54
0.12	1.38	2.90	3.38	2.72	1.72	1.11
0.97	0.99					

GAIN - LOADED APERTURES - OPTIMUM LOADS

3.02	2.76	2.09	1.32	0.75	0.58	0.88
1.74	3.24	5.14	6.58	6.47	4.47	1.74
0.12	0.31	1.20	1.34	0.61	0.07	0.28
0.79	0.94	0.72	0.46	0.37	0.47	0.76
1.21	1.64	1.80	1.60	1.20	0.83	0.64
0.61	0.62					

DISTANCES OF SHORTS FOR WAVEGUIDE LOADS - 50 DEGREES

SHORT(1) = 34.690 MM

SHORT(2) = 34.464 MM

SHORT(3) = 34.531 MM

SHORT(5) = 34.394 MM

SHORT(6) = 34.451 MM

SHORT(7) = 34.540 MM

SHORT(8) = 34.522 MM

REFERENCES

- [1] R. F. Harrington, R. F. Wallenberg, and A. R. Harvey, "Design of Reactively Controlled Antenna Arrays," Tech. Rept. No. 4, Contract No. N00014-67-A-0378-0006, Office of Naval Research, September 1975.
- [2] R. J. Coe and G. Held, "A Parasitic Slot Array," IEEE Transactions on Antennas and Propagation, January 1964, pp. 10-16.
- [3] R. F. Harrington and J. R. Mautz, "A Generalized Network Formulation for Aperture Problems," Tech. Rept. No. 13, Contract No. F19628-73-C-0047, Air Force Cambridge Research Laboratories, November 1975.
- [4] R. F. Harrington, "Time-Harmonic Electromagnetic Fields," McGraw-Hill Book Company, New York, 1961.
- [5] R. F. Harrington, "Field Computation by Moment Methods," Macmillan Company, New York, 1968.
- [6] E. Hallen, "Electromagnetic Theory," John Wiley and Sons, New York, 1962, p. 462.
- [7] D. R. Rhodes, "On the Stored Energy of Planar Apertures," IEEE Transactions on Antennas and Propagation, November 1966, p. 683.
- [8] R. F. Harrington and J. R. Mautz, "Reactively Loaded Directive Antennas," Tech. Rept. No. 1, Contract N00014-67-A-0378-0006, Office of Naval Research, Sept. 1974.
- [9] J. H. C. Van Heuven, "A New Integrated-Microstrip Transition," IEEE Transactions on Microwave Theory and Techniques, March 1976, pp. 144-147.
- [10] M. E. Davis, "Integrated Diode Phase-Shifter Elements for an X-Band Phased-Array Antenna," IEEE Transactions on Microwave Theory and Techniques, December 1975, pp. 1080-1084.
- [11] R. F. Harrington and J. R. Mautz, "Control of Radar Scattering by Reactive Loading," IEEE Transactions on Antennas and Propagation, Vol. AP-20, July 1972, pp. 446-454.
- [12] J. Luzwick and R. F. Harrington, "A Comparison of Optimization Techniques as Applied to Gain Optimization of a Reactively Loaded Linear Array," Tech. Rept. No. 1, Contract No. N00014-76-C-0225, Office of Naval Research, February 1976.

Jan 1974

DISTRIBUTION LIST FOR ONR ELECTRONICS PROGRAM OFFICE

Director Advanced Research Projects Agency Attn: Technical Library 1400 Wilson Boulevard Arlington, Virginia 22209	San Francisco Area Office Office of Naval Research 50 Fell Street San Francisco, California 94102
Office of Naval Research Electronics Program Office (Code 427) 800 North Quincy Street Arlington, Virginia 22217	Air Force Office of Scientific Research Department of the Air Force Washington, D. C. 20333
Office of Naval Research Code 105 800 North Quincy Street Arlington, Virginia 22217	Commanding Officer Office of Naval Research Branch Office 1030 East Green Street Pasadena, California 91101
Naval Research Laboratory Department of the Navy Attn: Code 2627 Washington, D. C. 20375	Commanding Officer Office of Naval Research Branch Office 495 Summer Street Boston, Massachusetts 02210
Office of the Director of Defense Research and Engineering Information Office Library Branch The Pentagon Washington, D. C. 20301	Director U. S. Army Engineering Research and Development Laboratories Fort Belvoir, Virginia 22060 Attn: Technical Documents Center
U. S. Army Research Office Box CM, Duke Station Durham, North Carolina 27706	ODDR&E Advisory Group on Electron Devices 201 Varick Street New York, New York 10014
Defense Documentation Center Cameron Station Alexandria, Virginia 22314	New York Area Office Office of Naval Research 207 West 24th Street New York, New York 10011
Director National Bureau of Standards Attn: Technical Library Washington, D. C. 20234	Air Force Weapons Laboratory Technical Library Kirtland Air Force Base Albuquerque, New Mexico 87117
Commanding Officer Office of Naval Research Branch Office 536 South Clark Street Chicago, Illinois 60605	Air Force Avionics Laboratory Air Force Systems Command Technical Library Wright-Patterson Air Force Base Dayton, Ohio 45433

Air Force Cambridge Research Laboratory

L. G. Hanscom Field
Technical Library
Cambridge, Massachusetts 02138

Naval Postgraduate School
Technical Library (Code 0212)
Monterey, California 93940

Harry Diamond Laboratories
Technical Library
Connecticut Avenue at Van Ness, N. W.
Washington, D. C. 20438

Naval Missile Center
Technical Library (Code 5632.2)
Point Mugu, California 93010

Naval Air Development Center
Attn: Technical Library
Johnsville
Warminster, Pennsylvania 18974

Naval Ordnance Station
Technical Library
Louisville, Kentucky 40214

Naval Weapons Center
Technical Library (Code 753)
China Lake, California 93555

Naval Oceanographic Office
Technical Library (Code 1640)
Suitland, Maryland 20390

Naval Training Device Center
Technical Library
Orlando, Florida 22813

Naval Explosive Ordnance Disposal Facility
Technical Library
Indian Head, Maryland 20640

Naval Research Laboratory
Underwater Sound Reference Division
Technical Library
P. O. Box 8337
Orlando, Florida 32806

Naval Electronics Laboratory Center
Technical Library
San Diego, California 92152

Navy Underwater Sound Laboratory
Technical Library
Fort Trumbull
New London, Connecticut 06320

Naval Undersea Warfare Center
Technical Library
3202 East Foothill Boulevard
Pasadena, California 91107

Commandant, Marine Corps
Scientific Advisor (Code AX)
Washington, D. C. 20380

Naval Weapons Laboratory
Technical Library
Dahlgren, Virginia 22448

Naval Ordnance Station
Technical Library
Indian Head, Maryland 20640

Naval Ship Research and Development Center
Central Library (Code L42 and L43)
Washington, D. C. 20007

Naval Ship Engineering Center
Philadelphia Division
Technical Library
Philadelphia, Pennsylvania 19112

Naval Ordnance Laboratory White Oak
Technical Library
Silver Spring, Maryland 20910

Naval Avionics Facility
Technical Library
Indianapolis, Indiana 46218